Acta Geologica Sinica (English Edition), 2019, 93(5): 1354–1376

Geochemical Characteristic of Charnockites in North Margin of North China Craton: Indicating the Significiant of the Neoarchean Tecnotic Event

SHI Qiang, FENG Fan, XU Zhongyuan*, LIU Zhenghong, DONG Xiaojie and LI Gang

College of Earth Sciences, Jilin University, Changchun 130001, China

Abstract: The Neoarchean charnockites of North margain of North China Craton (NCC) has become a hot topic into understanding the Early Precambrian basement. Although there is a broad consensus that charnockite is usually related to granulite facies metamorphism, whether its petrogenesis and tectonics characteristics remains controversial. Inclusions within hypersthene and garnet in charnockite are used to identify the peak granulite facies mineral assemblage, with the formation of Magnesian–charnockite attributed to anatexis of the protolith associated with this granulite facies metamorphism. The distribution of major and trace elements in charnockite is very uneven, significant depleted in LILEs (eg. Cs, U, Th) and HFSEs (eg. Nb, Ta, P and Ti), riched in Sr. Raising to the coexistence of Eu–enrichment and Eu–depletion type of REE patterns that influenced by the content of plagioclase and the remnants minerals of zircon and apatite. Comparative the petrography, geochemistry and geochronology data of Magnesian–charnockite indicate that the ratios of mafic pellites and basalts involved in anatectic melting are different by the upwelling of mantle magma, also resulting in the Eu anormals characteristics. The formation of the Magnesian–charnockite is closely connected with the subduction of the NCC oceanic crust (About ~2.5 Ga). However, Ferroan–charnockite may be the formed by the crystallization differentiation of the upwelling of mantle–derived shoshonitic magma (About ~2.45 Ga), with the lower crust material addition.

Key words: Neoarchean, Magnesian–charnockite, Ferroan–charnockite, Metamorphic anatexis event, NCC

Citation: Shi et al., 2019. Geochemical Characteristic of Charnockites in North Margin of North China Craton: Indicating the Significiant of the Neoarchean Tecnotic Event. Acta Geologica Sinica (English Edition), 93(5): 1354–1376. DOI: 10.1111/1755-6724.14384

1 Introduction

Charnockite has been considered as granitic rocks containing the orthopyroxene that formed under low water activity (or anhydrous) conditions by simulate phase equilibria of High–temperature and High–pressure (HTHP) melting experiments (Holland., 1900; Brown., 1994, 2004; Kriegsman., 2001; Le Maitre, 2002; Cheng et al., 2004). They are always discovered in precambrian high–grade metamorphic complex rocks. Recently years, Frost and Frost (2008) have redefined the charnockites as an orthopyroxene bearing granitic rocks of igneous rock origin or that are present as orthogneiss within a common constituent of granulite–facies metamorphic terrains or a metamorphic granulite facies of granite. They are usually showing spatial association of rocks of granulite. The origin and tectonic of the charnockites of NCC are remains debated, which has become a hot piont of the origin studies of the charnockites in Inner Mongolia (Wuchuan–Guyang charnockite), Hebei (Qianxi charnockite), and Shandong (Yishui charnockite) provinces, China. The origin and tectonic has concluded as follow: (1) Production of migmatite formed by the anatexis of wall rock (Wang et al., 1984; Qian et al., 1985; Sun et al., 1989; Su et al., 2003; Zhang et al., 2014); (2) Formation of the protolith of tonalite–granodiorite, with the enviorment of the granulite facies metamorphism and involving the CO_2–rich fluids (Geng et al., 1990); (3) Product of the crystallization differentiation (Wang et al., 1992); and (4) Partial melting of mafic crustal rocks (Ma et al., 2013a; Bai et al., 2015). The high–grade crustal of NCC, north margin of the between the Ordos Block and Yinshan Block, is characterized by anatectic charnockite and high–grade metamorphic complex. This anatectic charnockites mainly occurs in Shiguai–Baotou (Liu et al., 2017), Gonghudong–Guyang (Dong et al., 2012a; Ma et al., 2013a), Xiwulanbulang (Zhang et al., 2014; Shi et al., 2019a), Jining (Shi et al., 2019b, 2019c), Gehuyao (Zhang et al., 2017), Qian'an (Han et al., 2016) in Northern margin of NCC, and together with granulites, gneiss greenstone and khondalite belt, forming a significant component of the early precambrian metamorphic baseement (Fig. 1). A lot of geochemistry and Isotope chronology bearing on anatectic charnockite from the early precambrian basement of NCC is compiled here. According to a study of the geochemical characteristics of the anatectic charnockite samples are least likely to have been influenced by the metamorphism superposited. However, most acheivements of the previously studies on charnockites are carried out from the aspects of metamorphism evolution and isotopic chronology. Rajesh et al. (2004) and Rajesh (2012) attempted to study the petrogenesis and tectonic environment of charnockite by

* Corresponding author. E-mail: xuzy@jlu.edu.cn

http://www.geojournals.cn/dzxbcn/ch/index.aspx; https://onlinelibrary.wiley.com/journal/17556724

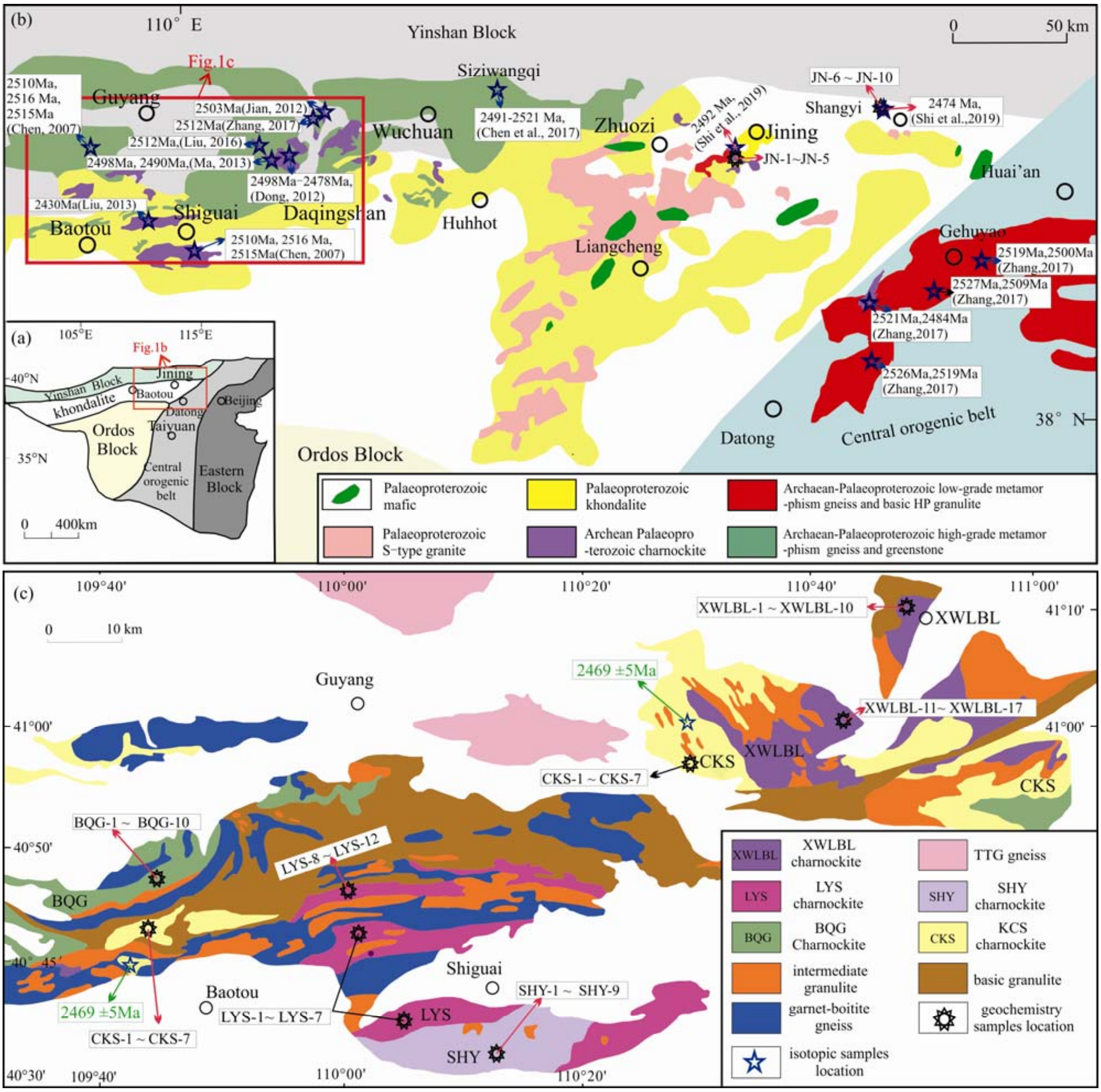

Fig. 1. Sketch map showing distribution of late Archean terranes in the NCC (after Zhao et al., 2005; Dong et al., 2012a; Ma et al., 2013a; Zhang et al., 2014; Liu et al., 2017), in which the position of Fig. 1b is indicated and published zircon ages (mostly SHRIMP and LA–ICP–MS) are compiled. Northern margin of the NCC Yinshan Block metamorphic Dating Statistics (Fig. 1b, Compiled after Zhao et al., 1998, 1999; Zhang et al., 2005; Tao and Hu, 2002; Jia et al., 2004; Jian et al., 2005; Ma et al., 2010). Detailed geological map of the Xiwulanbulang area and Sampling locations (Fig. 1c).

means of petrogeochemistry characteristics in South India. Basing on the previously Archean tectonic evolution models of NCC, the diference of geochemical characteristics of charnockite samples from different location{such as Shanheyuan (SHY) charnockite, Biqigou (BQG) charnockite, Cunkongshan (CKS) charnockite, Langyashan (LYS) charnockite, Xiwulanbulang (XWLBL) charnockite} are used to constraint on the formation of the nature continental crust with time. In the process, we compiled geochemical data of these charnockites to discuss and develop an understanding of the geochemical characteristics might be related to their source rocks, petrogenetic processes and tectonic environments.

2 Geological Background

The Early Precambrian metamorphic basement of NCC is separated into the Eastern Block, Western Block and Paleoproterozoic Trans–North China Orogen (Zhao et al., 2005). Western Block (Fig. 1a) is composed of the Yinshan Block, Khondalite belt and Ordos Block, and at the end of the Paleoproterozoic, all of them has integrated into a centralized cratonic framework. It is well known that Yinshan block is the largest and integrated area of early precambrian metamorphic in the western block, locating in NCC, with a ductile shear zone of south side bounded by the Xia Shihao–Jiu Guan ductile that output to East–West trending (Zhao et al., 1999, 2003, 2005). Yinshan Block is the largest and most complete area of Archean basement in the Western Block, located on the northern margin of the NCC, with the south side bounded by the Xia Shihao–Jiu Guan ductile east–west trending Xia–Shihao–Jiu–Guan ductile shear zone. Most of these basement rocks have characteristics of upper greenstone to lower–amphibolite facies metamorphism, and the metamorphic complex rocks also experienced high–grade metamorphism, generally of the high amphibolite to granulite facies (Jin et al., 1991, 1994). The paleoproterozoic khondalite belt is in the southern side of the Xiashihao– JiuGuan large–scale ductile shear zone (Fig. 1b). The upper part of the greenstone belt sequence comprises meta–komatiite and volcano–sedimentary rocks (Chen, 2007; Jian et al., 2012), granitic rocks from the upper Greenstone Belt is consists of TTG gneisses (Jian et al., 2005; Ren et al., 2010; Jian et al., 2012) and sanukite (Jian et al., 2012; Ma et al., 2013a). Occuring a dome structure consists of granulite and charnockite in the high–grade metamorphic complex rocks, it is also exposed mainly in the Baotou–Wuchuan–Guyang–Jining–Gehujiao area (Zhang et al., 2005; Ma et al., 2013a; Liu et al., 2017). Zircon dating of these rocks of the charnockites (XWLBL–JN Charnockite) and TTG gneisses (Wuchuan–Guyang–Siziwangqi area Gneisses) have affirmed that the metamorphic intrusive rocks from the North margian of NCC are more possibly formed in the Neoarchean (Dong et al., 2012a; Jian et al., 2012; Ma et al., 2013a; Zhang et al., 2014; Shi et al., 2019a). Previously study have shown that metamorphic origin zircon dating from the Greenstone belt, TTG and high–grade metamorphic complex obtained the metamorphic ages of 2.55–2.50 Ga (Jian et al.,2005, 2012; Ma et al., 2013a. 2013b; Wang et al., 2015; Liu et al., 2017; Chen et al., 2017). There are also some Neoarchean– Paleoproterozoic high–grade metamorphic complex rocks widely distributed in the khondalite series Belt and Yinshan Block, more and more studies have shown the metamorphic ages of ~2.5 Ga and ~1.95 Ga are widespread of the NCC (Jian et al.,2005, 2012; Ma et al., 2013a. 2013b; Wang et al., 2015; Liu et al., 2017; Guo et al., 2001; Wang et al., 2005; Wan et al., 2006, 2009, 2011, 2013a, 2013b, 2015; Santosh et al., 2006, 2007a, 2007b; Xu et al., 2011; Dong et al., 2013; Cai et al., 2014; Ma et al., 2015; Chen et al., 2017; Shi et al., 2018, 2019a, 2019b, 2019c).

Granulitic units are composed of granulite and high–grade metamorphic gneisses that have been retrogressed, both of which are closely associated with anatectic charnockite (Fig. 1c). Anatectic charnockite and gneisses are present in the NCC as irregularly shaped or banded units scattered throughout the localities of Jining Sanchakou (JN Charnockite), Baotou Shiguai (SHY Charnockite and LYS Charnockite), Guyang (BQG Charnockite and CKS Charnockite), Xiwulanbulang (XWLBL Charnockite), however, some charnockites might be related to mantle sources magmatic generates melting (Yang et al., 2014; Shi et al., 2019). The Neoarchean charnokite of Yinshan Block has been a hot topic into understanding the precambrian geology of the NCC. Although there is a broad consensus that the charnokite is usually related to granulite facies metamorphism, whether its petrogenesis and tectonics still remains controversial. Previous study has shown that the charnockite–granulite and other anatectic original rocks are closely distribution along to each other in spatially (Zhang et al., 2014; Shi et al., 2019a). We are also found that there are also two types hypersthene in NCC Charnockite (this paper): ① First type, with the characteristics of irregular in shape and xenomorphic structure, indicating a metamorphism origin. ② Second type, the hypersthene has the feature of tabular structure, without a obviously xenomorphic structure, referring to a magmatic origin. The purpose of our study is to contrast the geochemical and geochronology of these rocks to the existing high–grade metamorphic rocks research achievements which collected from the nearby combination in order to better understand the evolution of the charnockites in the NCC. Comparing our results to those charnockite bodies reported in the Southern India where has a very mature understanding of the origin, material source of charnockite and revealing the contribution on regional tectonic evolution.

3 Charnockite Petrography in NCC

The hypersthene (1–5%) of SHY Charnockite is irregular in shape and tabular structure, with partly hypersthene has a porphyritic texture. Biotite (1–5%) is fine flake, both are surrounding the hypersthene. Plagioclase (55–65%) has the characteristics of polysynthetic twins, with an irregular granular in shape, and it is also interstitial to hypersthene and biotite. Microcline (20–35%) always surrounds the hypersthene obviously. Quartz (15–20%) has an irregular serrated and resorbed grain boundaries characteristic, showing a granular texture and encircling the hypersthene (Fig. 2b).

BQG Charnockite has a typical mineral assemblage of plagioclase (35–40%), microcline (15–20%), hypersthene (5–10%), biotite (5–10%) and quartz (15–20%). Hypersthene occur as subhedral short columns, with pyroxene chain, part of them retrograded to biotite. Showing a typical xenomorphic granular structure with quartz and plagioclase peritectic. Plagioclase displaying polycrystalline twins. Microcline has hypidiomorphic xenomorphic granular structure (Fig. 2d).

The garnet (1–5%) of LYS Charnockite also has a typical xenomorphic granular structure, surrounded by hypersthene and irregular quartz. Hypersthene (1–5%) has irregular granular structure, usually symbiosis with iregular granular quartz, surrounded by the garnet. And showing xenomorphic structure with quartz and plagioclase peritectic. Plagioclase (30–40%) displaying polycrystalline twins characteristics. Microcline (15–20%) has hypidiomorphic–xenomorphic granular structure. The quartz (15–20%) has a granular texture characteristic, with an irregular serrated. Hornblende (1–5%) has an iregular

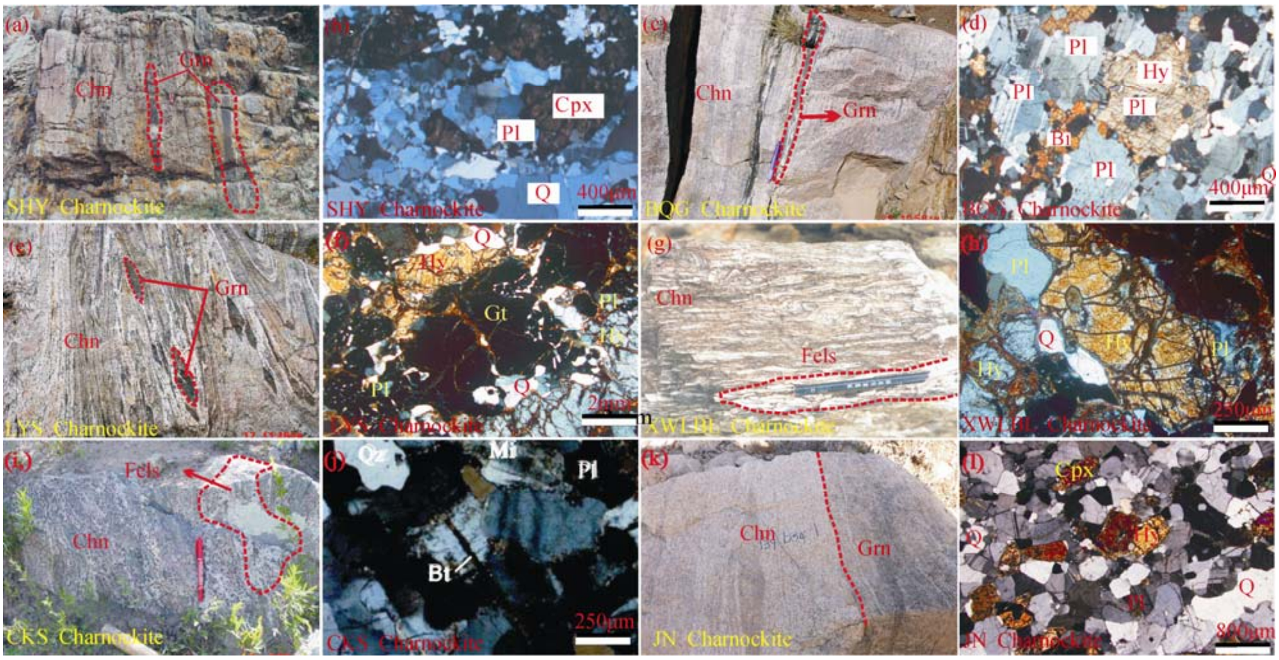

Fig. 2. The contact between charnockite and granulite, Granulite inclusions in charnockite, the gradational contact between charnockite and granulite, and part of granulite retrogressed to amphibolite of NCC Charnockite (SHY Charnockite, BQG Charnockite, LYS Charnockite, CKS Charnockite, JN Charnockite) in the field. (eg. 2a, 2c, 2e, 2k). Banded leucosome and melanosome in charnockite. (eg. b, d, f, h, j, l) Optical photomicrographs of charnockite (SHY Charnockite, BQG Charnockite, LYS Charnockite, CKS Charnockite, JN Charnockite).

Abbreviations are as follows: Chn = charnockite; Grn = granulite; Fels = leucosomes; Hy = hypersthene; Mi = Microcline; Pl = plagioclase; Q = Quartz; Opx = Orthopyroxene; Cpx = clinopyroxene; Hb = hornblen.

texture, aways surrounded by hypersthene (Fig. 2f).

CKS Charnockite has a mineral assemblage of plagioclase (15–25%), microcline (45–55%), hypersthene (1–5%), biotite (1–5%) and quartz (15–30%). Hypersthene also has xenomorphic structure, with the quartz and plagioclase peritectic. Plagioclase also displaying polycrystalline twins. Microcline has hypidiomorphic or xenomorphic granular structure, encircling the plagioclase and quartz (Fig. 2j).

The hypersthene (5–10%) of JN Charnockite has the xenomorphic structure with quartz and plagioclase peritectic, in which irregular in shape and has the tabular structure, occuring with granular quartz and partly hypersthene has a porphyritic texture (Fig. 2l). Plagioclase (50–55%) is irregular in shape, with the polysynthetic twins. Microcline (15–25%) surrounds the hypersthene. Quartz (10–15%) has a irregular and serrated characteristics, usually encircling the hypersthene and feldspar (Fig. 2l).

XWLBL Charnockite is composed of the mineral assemblage of hypersthene (5–10%), garnet (1–5%), plagioclase (35–40%), microcline (10–15%) and quartz (15–20%). Garnet has the feature of xenomorphic structure, surrounded by irregular quartz and hypersthene. Hypersthene has a feature of irregular granular in shape, occuring with the irregular granular quartz characteristics, and all of them are surrounding by the garnet (Fig. 2h). Plagioclase has an irregular granular in shape, interstitialing to hypersthene and garnet. Microcline also surrounds the hypersthene (Fig. 2h). Quartz has a feature of irregular serrated and resorbed grain boundaries, encircling the hypersthene and feldspar (Fig. 2h).

4 Analytical and Methods

The compositions of major–element of charnockite samples were tested on the Axios X–ray fluorescence spectrometer at the China National Research Center for Geoanalysis, Beijing, China. The trace–element analyses were measured on an Elan 9000 ICP–MS (Inductively Coupled Plasma–Mass Spectrometer), mading in the PerkinElmer company of United States in USA, and the accuracy of analysis is better than 10%. Geochemistry compositions and analytical standard samples for each major and trace element are given in Supplementary Table 3.

5 Results

5.1 Effect of metamorphic superimposed

A detailed geochemical study of Nagercoil charnockites in southeastern India affected by the superimposed metamorphism of late Neoproterozoic–Precambrian granulite facies metamorphic is carried out (Rajesh et al., 2011, 2012). Considering the influence from the later metamorphic superimposed, a geochemical comparative study of low–Sr Nagercoil charnockite samples was made with that of the dehydration zones of the Opx (orthopyroxene) bearing metamorphic, occurring in gneisses from southern India and other areas (Figs. 3, 4).They are also considered to represent in situ stages of granulite formation driven by the influx of low–aH_2O fluids. According to the content of Sr of NCC charnockite can be divided into two types of High Sr (Fig. 3, Sr: 518–911 ppm) and Low Sr (Fig. 3, Sr: 143–416 ppm). Among them, high–Sr and low–Sr charnockites have a similar SiO_2 content (60–74 wt%), at the same SiO_2 content condition, high–Sr anatectic charnockite is relatively enriched with Al_2O_3, K_2O and Na_2O, FeO^T, Rb, depleted in Nb (Fig. 4). High–Sr anatectic charnockite has the characteristics of trondhjemite–tonalite–granodiorite in An–Ab–Or diagram, however, most samples of low–Sr charnockite has the characteristics of tonalite–granodiorite–monzonitic granite (Fig. 5). The characteristics of low–Sr charnockite with high K_2O and Nb contents are closely related to previous geochemical studies. It is demonstrated that potassium plays an important role in the formation of some dehydrated metamorphic zones (Figs. 4c, 4d, Stahle et al., 1987; Raith and Srikantappa, 1993). It is also very similar to the characteristics of high–Sr charnockite in southern India studied by Rajesh et al (2011).

Geochemical characteristics indicate that low–Sr charnockite may be related to later metamorphism, whereas high–Sr charnockite were most likely not affected by late metamorphism. The results of geochronology show that the charnockites in the early Precambrian basement are widely affected by the post–metamorphism, and The study results of the geochronology show that the charnockites in the early Precambrian basement are widely affected by the post–metamorphism, and it is related to the regional metamorphism of the northern margin of the NCC at ~2.45 Ga , ~1.95 and ~1.85 (Li et al., 2000; Zhao et al, 2005; Dong et al., 2007; Jian et al., 2008; Wan et al., 2008; Li et al, 2011; Jian et al., 2012; Ma et al., 2013a; Ma et al., 2013b; Ma et al., 2013c; Guo et al, 2012; Liu et al., 2013; Cai et al., 2014; Bai et al., 2015; Xu et al., 2015; Ma et al., 2016; Yang et al., 2016; Shi et al., 2018). Therefore, we selected high Sr samples for corresponding study.

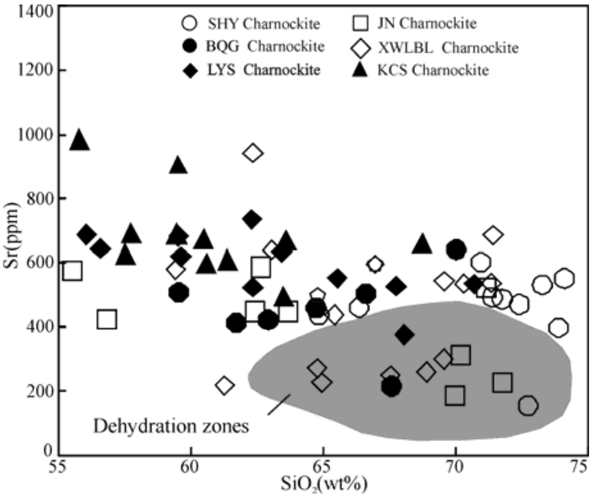

Fig. 3. The charnockites of North margin of NCC SiO_2 vs. Sr diagram. See Rajesh et al. (2011) for references used to compile the compositional range of orthopyroxene–bearing metamorphic dehydration zones.

Lower SiO_2 content samples(<60 wt%) are aimed for comparing with higher samples(>60 wt%) in the Fig. 3, 4, 6, 8, 9, 11a, 12a, 16a, however, they are removed in Fig. 5, 7, 10, 11b, 12b, 13, 14, 15, 16b, 17.

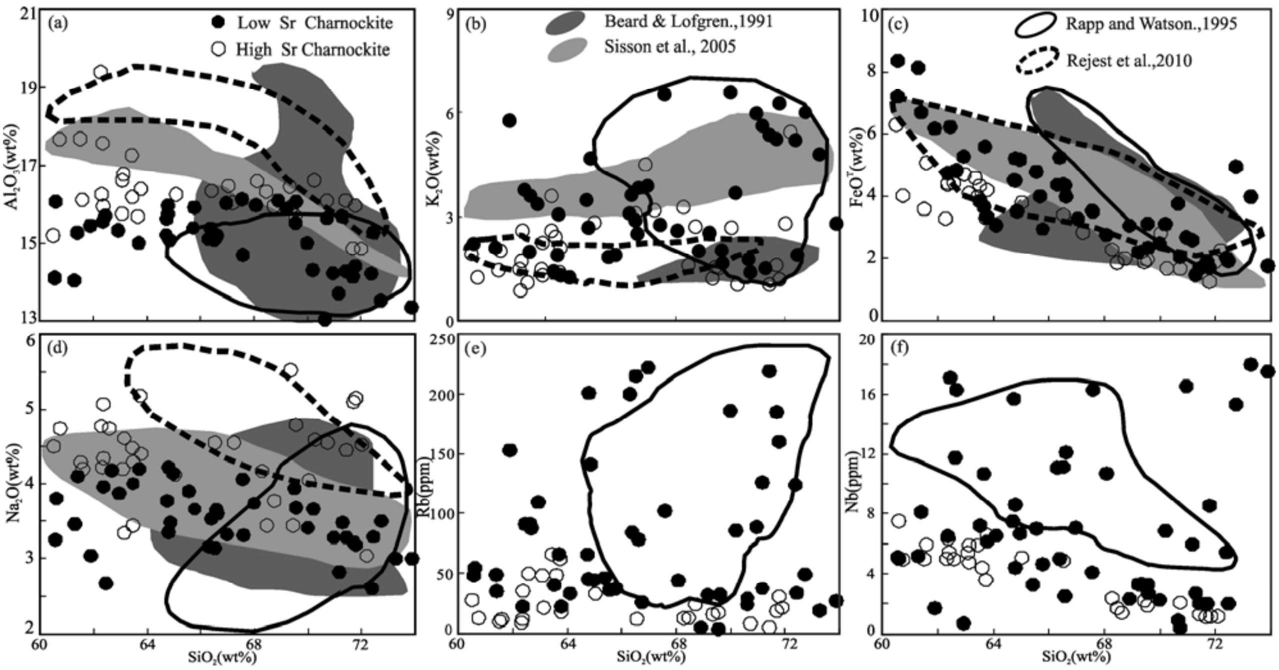

Fig. 4. The Hark diagram of North margin of NCC high–Sr and low–Sr charnockites.

Amphibolite dehydration melts (only those with comparable P–T conditions to the Nagercoil charnockites are plotted) from Beard & Lofgren (1991) and Rapp & Watson (1995), and high–temperature hydrous basalt melts from Sisson et al. (2005) are shown for comparison. The compositional range of dehydration zones (metamorphic incipient charnockites) in gneisses from southern India and elsewhere are from Janardhan et al. (1982), Hansen et al. (1987), Yoshida et al. (1991), Dobmeier and Raith (2002), Harlov et al. (2012). For clarity, garnet–bearing and garnet–absent charnockites are not distinguished.

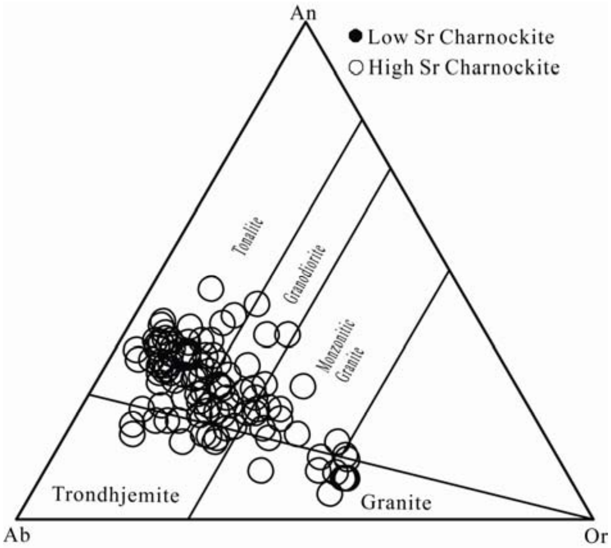

Fig. 5. The An–Ab–Or diagram of North margin of NCC high–Sr and low–Sr charnockites.

5.2 Geochemical characteristics of charnockites

Comparison and analysis of geochemical data of charnockites from different locations of the world, such as the Magnesian–charnockite has the calcic to calc–alkalic and metaluminous group characteristics; However, the Ferroan–charnockite has the feature of alkali–calcic to alkalic and metaluminous group, and also having a transitional group that straddles from ferroan to magnesian group (Rajesh and Santosh, 2004; Frost and Frost, 2008; Rajesh, 2012). Generally speaking, Ferroan–charnockite is more likely occurred in an extensional tectonic environment (Frost and Frost, 2008; Rajesh, 2012; Rajesh and Santosh, 2012), however, the Magnesian–charnockite is more possibly occurred in a magmatic arc setting (Emslie, 1991; Frost et al., 2001; Keppie et al., 2003; Rajesh et al., 2011). The geochemical characteristics of charnockite in different areas of the northern margin of the NCC are roughly similar, but they still have own unique characteristics. The magmatism of charnockite of older can only consider high Sr samples which have not been affected by metamorphism superimposed. According to the characteristics of rare earth element Eu anomaly characteristics, high Sr samples of charnockite can be divided into two types: Eu enrichment and Eu depletion. The ratio of A/CNK is 0.52–1.24, with metaluminous to weak peraluminium characteristics (Fig. 11).

SHY Charnockite mainly located in the north margin of NCC, South of the Shiguai and near Shanheyuan area (Fig. 1b, Sample Number from SHY–1 to SHY–9), and most of the samples have magnesian charnokite characteristics (Fig. 6, $FeO^T/(FeO^T+MgO)$: 0.64–0.96), prossesing a partition curve of Eu–enrichment type (Table 1, Eu/Eu*: 1.07–3.18, $FeO^T/(FeO^T+MgO)$: 0.80–0.96, Magnesian charnokitess) and Eu–depletion type (Table 1, Eu/Eu*: 0.35–0.95, $FeO^T/(FeO^T+MgO)$: 0.64–0.77, Ferroan charnokitess) obviously. The An–Ab–Or diagram shows that the Eu enrichment type has the characteristics of granodiorite–monzogranite, and the Eu depletion type has granite characteristics (Fig. 7). Compering with Eu–depletion type, Eu–enrichment type samples are relatively enriched in Al_2O_3, MgO, CaO, P_2O_5, and depleted in FeO^T, Na_2O, K_2O, Na_2O, Nb, Rb (Fig. 8). Eu enrichment type samples has the characteristic of the Calclic to Calclic –Alkline series, Eu–depletion type samples have Calclic–Alkline to Alkline–Calclic, all of them have potassium characteristics. The total REE content is relatively high in samples with low Eu/Eu* values (Fig. 10b, Table 1; Eu enrichment type ΣREE: 54.24–160.03ppm; Eu–depletion

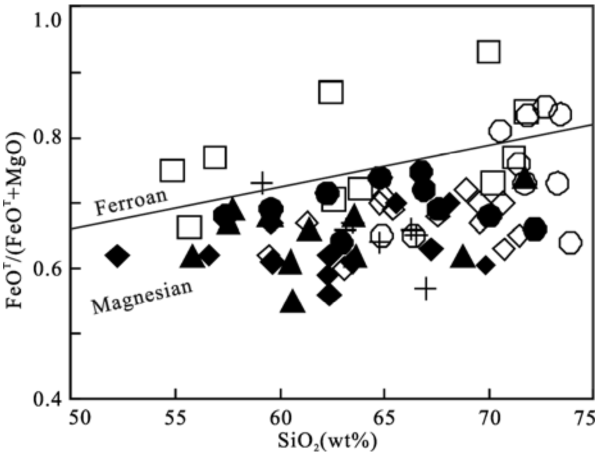

Fig. 6. The SiO_2 vs. $FeO^T/(FeO^T+MgO)$ diagram of Eu enrichment type and Eu depletion type charnockite samples from the north margin of NCC (Frost, 2001; Rajesh, 2012; Rajesh and Santosh, 2012). The legend is the same as Fig. 3.

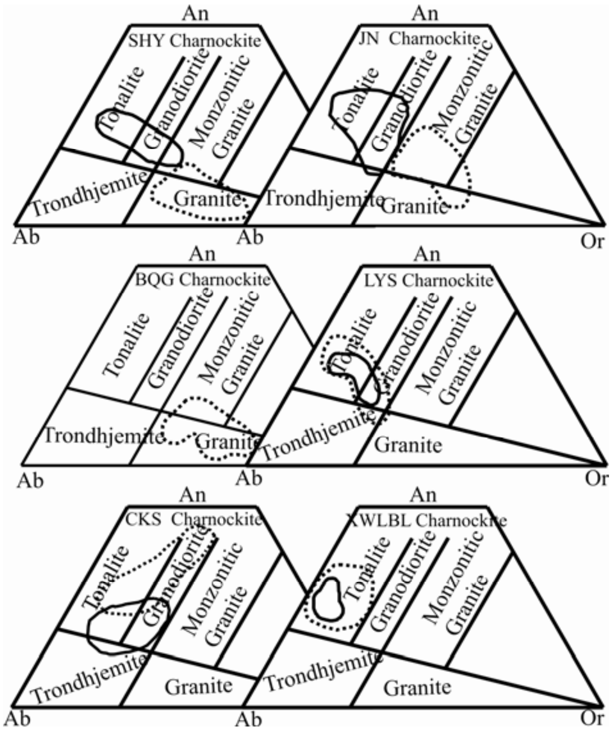

Fig. 7. The An–Ab–Or diagram of Eu enrichment type and Eu depletion type charnockites samples from the north margin of NCC (O'Connor., 1965).

Solid lines represent Eu enrichment type samples, dotted line represent Eu enrichment type samples.

type ΣREE: 149.10–370.76 ppm), and all of them has the characteristic of HREE depletion obviously. The total content of trace elements is very similarity (Fig. 10a), all of them enrichment in LILEs (eg. K, Rb, Ba), depleted in HFSEs (eg. Nb, Ta, P and Ti). Specially, the Eu–enrichment type samples riched in HPEs (eg. Th), more depleted in LILE (eg. Rb and Ba), and more depleted in partial HFSEs (eg. Ti). The ratio of A/CNK is 0.87–1.10, with the characteristic of metaluminous to weak peraluminium (Fig. 11b).

BQG Charnockite mainly located in the north margin of NCC, North–West of the Baotou and near Biqigou area (Fig. 1b, Sample Number from BQG–1 to BQG–10), and the samples have magnesian charnokites characteristics (Fig. 6; $FeO^T/(FeO^T+MgO)$: 0.66–0.76), prossesing a partition curve of Eu–depleted type. The An–Ab–Or diagram shows that the Eu–depletion type has granite–monzonitic granite characteristics. Compering with other Eu–enrichment type charnockites, Eu–depletion type samples are relatively depleted in Al_2O_3, CaO, Na_2O, and enriched in FeO^T, MgO, K_2O, P_2O_5, TiO_2, Nb, Rb (Fig. 8). Eu–enrichment type samples has the characteristic of the Calclic–Alkline to Alkline series. The total REE content is relatively high in samples with low Eu/Eu* values, Eu–depleted type (Fig. 10d, ΣREE: 104.93–481.31 ppm), and all of them has the characteristic of LREE enrichment and HREE depletion obviously. About the trace elements (Fig. 10c), similar to other Eu –depletion type samples, all of them more enrichment in LILEs (eg. K, Rb, Ba), and depleted in HFSEs (eg. Nb, Ta, P and Ti), and more depleted in partial HFSEs (eg. Ti). The ratio of A/CNK is 0.87–1.08, with the characteristic of metaluminous to weak peraluminium (Fig. 11b).

LYS charnockite mainly located in the north margin of NCC, South–east of the Baotou and near Shiguai area (Fig. 1b, Sample Number from LYS–1 to LYS–12), and most of the samples have Magnesian–charnokite characteristics (Fig. 6, FeO^T/FeO^T+MgO: 0.41–0.70), prossesing a partition curve of Eu–enrichment (Fig. 10f, Table 1, δEu: 1.04–4.39, $FeO^T/(FeO^T+MgO)$: 0.41–0.70) and Eu–depletion type (Fig. 10f, Table 1, δEu: 0.57–0.94, $FeO^T/(FeO^T+MgO)$: 0.56–0.67). The An–Ab–Or diagram shown that the Eu–enrichment type has the characteristics of granodiorite–tonalite, the Eu–depletion type has trondhjemite–granodiorite–tonalite characteristics (Fig. 7). Compering with other Eu–enrichment type charnockites, Eu–depletion type samples are relatively depleted in Al_2O_3, Na_2O, CaO, Ba, Rb, and enriched in FeO^T, MgO, K_2O, Nb (Fig. 8). Eu–enrichment type samples has the characteristic of the Calclic series, Eu–depletion type samples has Calclic to Alkline–Calclic. The content of total REE is relatively high in samples with low Eu/Eu* values (Fig. 10f, Eu–enrichment type ΣREE: 39.91–99.8 ppm; Eu–depletion type ΣREE: 77.19–109.18ppm), and all of them has the characteristic of HREE depletion obviously. About the trace elements (Fig. 10e), the total content of Eu–enrichment and Eu–depletion type is very similarity, all

Table 1 Geochemical characteristics of charnockite in the northern margin of NCC

Geochemical		Numbers	Eu/Eu*	SiO_2 (wt%)	CaO (wt%)	CaO+Na_2O (wt%)	FeO^T (wt%)	K_2O (wt%)	K_2O/Na_2O	K_2O+Na_2O (wt%)	TiO_2 (wt%)	Nb (ppm)	ΣREE (ppm)	$(La/Yb)_N$	$Mg^\#$	HFSE	LILE
SHY Charnockite	Eu enrichment	5	1.07–3.18	70.3–73.9	1.64–2.61	4.28–5.61	1.62–3.26	2.80–5.36	0.93–2.00	5.80–8.64	0.25–0.48	2.0–30.0	54.2–160.0	17.5–77.4	34.6–40.0	Low Th	Low Sr High K
	Eu depletion	4	0.35–0.95	64.4–73.3	3.48–5.11	3.49–4.72	1.91–5.25	3.61–6.57	1.02–2.42	6.50–9.50	0.15–0.57	2.0–18.0	149.1–370.8	10.8–92.9	7.33–48.7	High Th	High Sr Low K
BQG Charnockite	Eu depletion	8	0.45–0.99	57.4–72.2	1.30–4.77	4.34–9.14	2.80–7.40	2.50–5.77	0.66–1.98	6.39–8.11	0.30–1.10	0.7–16.0	104.9–481.3	13.5–50.4	36.3–48.9	–	–
XWLBL Charnockite	Eu enrichment	8	1.24–3.62	65.4–71.4	4.00–5.43	4.43–6.45	1.67–3.54	0.41–1.13	0.09–0.26	4.67–6.04	0.04–0.48	0.9–4.1	40.68–56.23	13.5–45.0	44.0–54.0	Low U, Th	Low K High Sr
	Eu depletion	8	0.60–0.96	59.4–64.8	5.07–6.76	7.62–9.33	4.38–8.14	0.52–1.63	0.16–0.53	3.98–6.13	0.43–0.67	4.4–8.0	75.2–220.3	15.7–74.8	45.0–57.0	High U,Th	High K Low Sr
LYS Charnockite	Eu enrichment	6	1.28–4.39	62.3–72.8	3.48–5.11	7.62–9.33	0.85–3.73	3.61–6.59	1.02–2.44	6.50–9.52	0.06–0.59	5.0–9.5	112.2–160.5	14.8–27.2	41.9–71.9	Low U,Th	High K Low Sr
	Eu depletion	6	0.67–0.94	59.6–62.4	5.28–5.89	9.24–10.39	2.12–3.2	2.80–5.39	0.93–2.03	5.80–8.67	0.23–1.15	5.9–15.0	112.2–160.6	12.9–19.5	40.0–57.9	High U,Th	Low K High Sr
CKS Charnockite	Eu enrichment	10	1.24–4.41	57.5–71.7	3.06–5.07	6.44–9.45	1.74–7.52	3.68–6.58	1.01–1.99	6.44–9.45	0.22–0.86	3.3–9.3	56.8–112.7	13.5–45.0	44.0–59.0	High Th	High K Low Sr
	Eu depletion	5	0.92–1.0	62.3–70.3	3.5–13.7	5.06–7.09	3.52–10.6	0.84–2.59	0.19–0.58	5.06–7.09	0.28–1.26	3.8–7.6	107.6–168.2	4.0–12.6	45.0–62.0	Low Th	Low K High Sr
JN Charnockite	Eu enrichment	5	1.07–1.90	62.5–71.8	1.25–3.78	4.43–6.45	1.69–3.11	3.68–6.58	1.01–1.93	7.34–9.99	0.30–1.39	2.2–17.0	135.5–372.5	19.1–54.2	14.0–43.0	High U,Th	High K Low Sr
	Eu depletion	5	0.49–0.94	54.9–67.3	3.11–6.73	7.31–11.41	4.83–9.26	1.20–3.60	0.26–1.20	5.61–7.25	0.74–1.69	15.0–20.0	236.4–389.5	6.2–18.1	37.0–47.0	Low U, Th	Low K High Sr

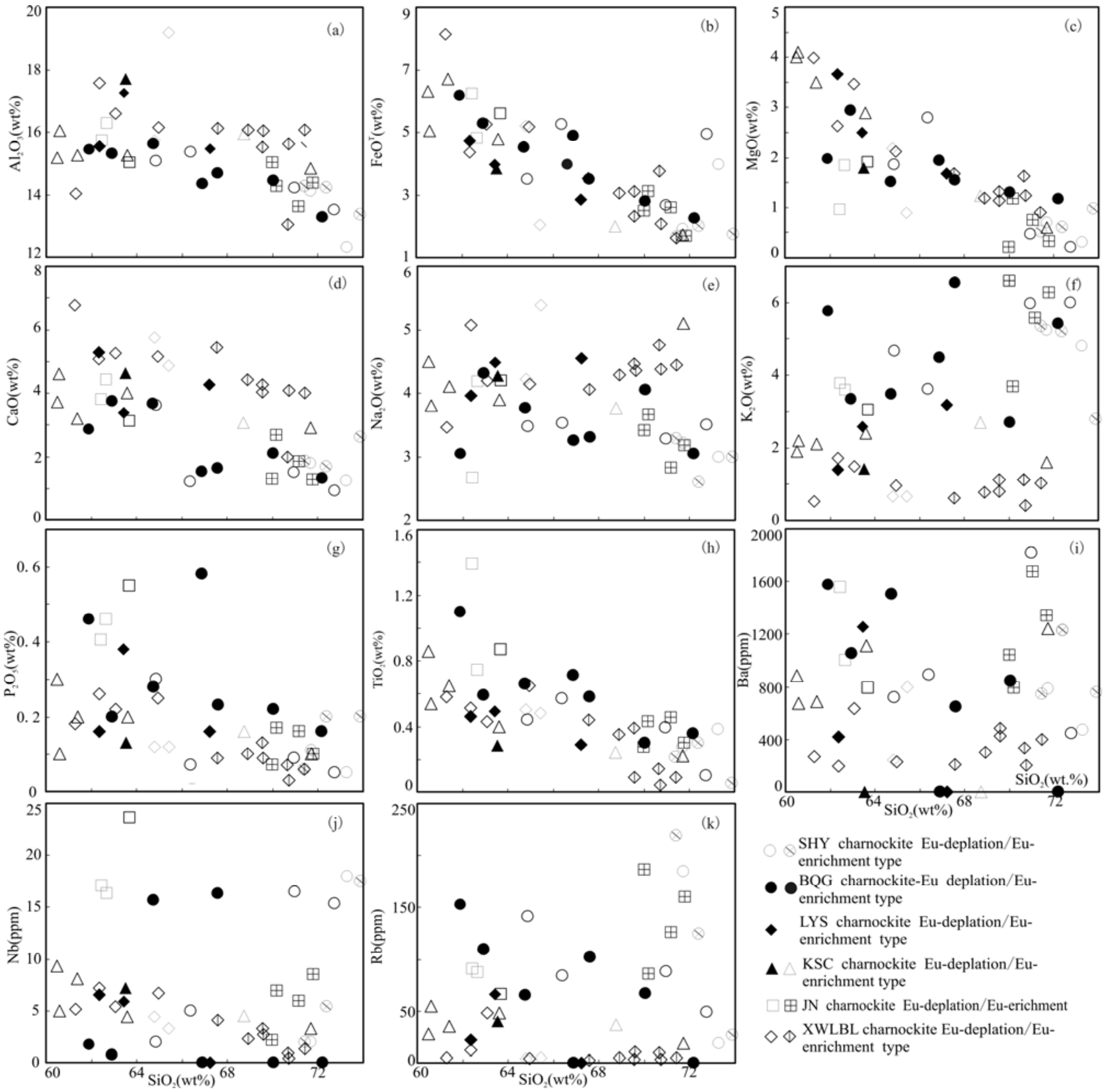

Fig. 8. The Hark diagram of Eu–enrichment type and Eu–depletion type charnockite samples from the north margin of NCC.

of them enrichment in LILEs (eg. K, Rb, Ba), depleted in HFSEs (eg. Nb, Ta, P and Ti). Specially, the Eu–enrichment type (Fig 10f) sample enriched in HPEs (eg. Th), more depleted in partial LILEs (eg. Rb and Ba) and HFSEs (eg.Ti). The ratio of A/CNK is 0.70–1.06, with the characteristic of metaluminous to weak peraluminium (Fig. 11b).

CKS Charnockite mainly located in the north margin of NCC, west of the Baotou and near Cunkongshan area (Fig. 1c, Sample number from CKS–1 to CKS–15), most of the samples have Magnesian–charnockite characteristics (Fig. 6, FeO^T/FeO^T+MgO: 0.52–0.74), prossesing a partition curve of Eu–enrichment type (Fig. 10j, δEu: 1.24–4.41, $FeO^T/(FeO^T+MgO)$: 0.55–0.74) and Eu–depletion type (Fig. 10j, δEu: 0.92–1.0, $FeO^T/(FeO^T+MgO)$: 0.51–0.68). The An–Ab–Or diagram shows that the Eu–enrichment type has the characteristics of trondhjemite–granodiorite–tonalite, and the Eu–depletion type has granodiorite–tonalite characteristics (Fig. 7). Comparing with other Eu–enrichment type charnockite, Eu depletion type samples are relatively depleted in FeO^T, MgO, K_2O, Nb, and enriched in Al_2O_3, Na_2O, CaO, Ba, Rb (Fig. 8). Eu–enrichment type samples has the characteristic of the Calclic series, Eu–depletion type sample has Calclic to Alkline–Calclic. The total REE content is relatively high in samples with low Eu/Eu* values (Fig. 10h, Eu–enrichment type ΣREE: 56.83–112.65 ppm; Eu–depletion type ΣREE: 107.56–168.18 ppm), and all of them has the characteristic of HREE depletion obviously. About the trace elements (Fig. 10g), the total content of Eu

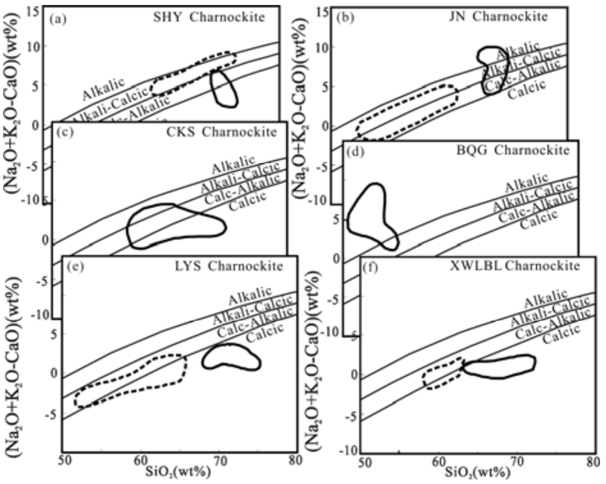

Fig. 9. The diagrams of the SiO_2 vs. (Na_2O+K_2O–CaO) Eu –enrichment type and Eu–depletion type charnockite samples from the north margin of NCC (Frost et al., 2001).

enrichment and Eu depletion type are very similarity, all of them enrichment in LILEs (eg. K, Rb, Ba), and depleted in HFSEs (eg. Nb, Ta, P and Ti). Specially, the Eu–enrichment type sample (Fig. 10h) enriched in HPEs (eg. Th), more depleted in partial LILE (eg. Rb and Ba) and partial HFSEs (eg. P and Ti). The ratio of A/CNK is 0.76–1.08, with the characteristic of metaluminous to weak peraluminium (Fig. 11b).

JN Charnockite mainly located in the north margin of NCC, Jining area (Fig. 1b, Sample Number from JN–1 to JN–10), most of the samples have Ferroan–charnockite characteristics (Fig. 6, FeO^T/FeO^T+MgO: 0.69–0.93), prossesing a partition curve of Eu–enrichment type (Fig. 1j, δEu: 1.07–1.90, FeO^T/ (FeO^T+MgO): 0.73–0.93) and Eu–depletion type (Fig. 10j, δEu: 0.49–0.94, FeO^T/ (FeO^T+MgO): 0.69–0.77). The An–Ab–Or diagram shows that the Eu–enrichment type has the characteristics of granodiorite–tonalite, and the Eu–depletion type has granodiorite–tonalite characteristics (Fig. 7). Compering with other Eu–enrichment type charnockite, Eu depletion type samples are relatively depleted in Al_2O_3, K_2O, Ba, Rb, and enriched in FeO^T, MgO, Na_2O, CaO, P_2O_5, TiO_2, Nb (Fig. 8). The Eu–enrichment type samples has the characteristic of the Calclic series, Eu–depletion type samples has Calclic to Calclic–Alkline. The total REE content is relatively high in samples with low Eu/Eu* values (Fig. 10j, Eu enrichment type ΣREE: 135.52–372.49 ppm; Eu depletion type ΣREE: 236.35–389.50 ppm), and all of them has the characteristic of HREE depletion obviously. About the trace elements (Fig. 10k), the total content of Eu–enrichment and Eu depletion type are very similarity, all of them enriched in LILEs (eg. K, Rb, Ba), and depleted in HFSEs (eg. Nb, Ta, Nd, P and Ti). Specially, the Eu–enrichment type sample (Fig. 10i) enriched in HFSEs (eg. Th), more depleted in LILEs (eg. K, Rb and Ba) and partial HFSEs (eg. Ta, P and Ti). The ratio of A/CNK is 0.84–1.02, with the characteristic of metaluminous to weak peraluminium (Fig. 11b).

XWLBL Charnockite mainly located in the north margin of NCC, west of the Wuchuan and near

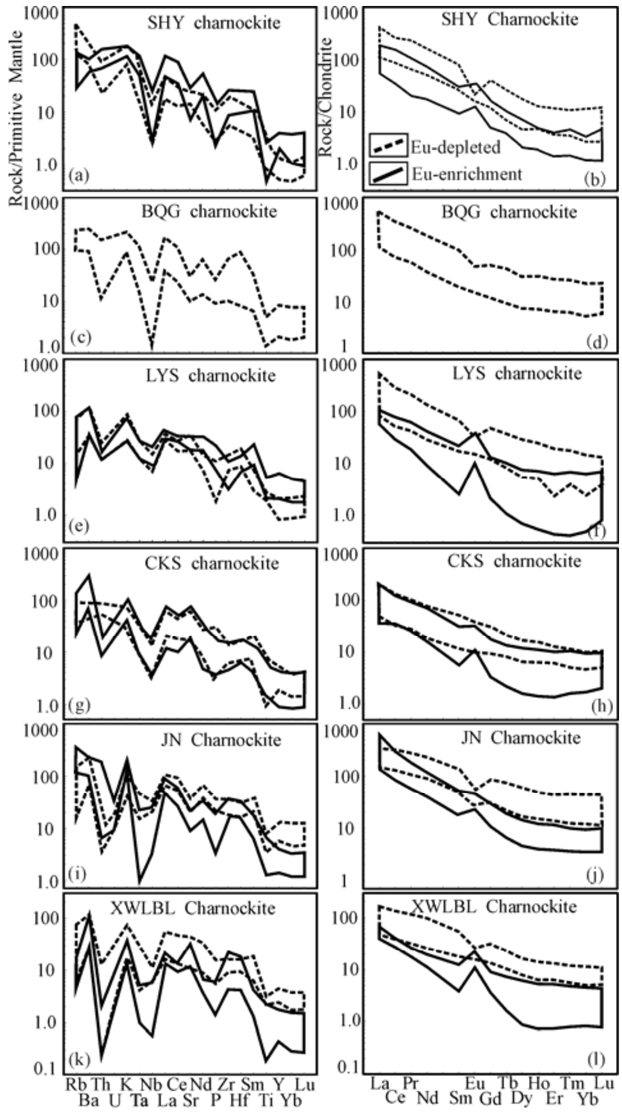

Fig. 10. The primitive mantle–normalized trace element spidergrams (left) and the Chondrite–normalized REE patterns (right) (Normalization values after Sun and McDonough, 1989) in Eu enrichment type and Eu depletion type charnockites samples from the north margin of NCC (Data from Chacko et al.,1992; Beard et al., 1991).

Xiwulanbulang (Fig. 1b), most of the samples have Magnesian–charnockite characteristics (Fig. 6, FeO^T/ FeO^T+MgO: 0.56–0.72), prossesing a partition curve of Eu–enrichment type (Fig. 10l, δEu: 1.24–3.62; FeO^T/ (FeO^T+MgO): 0.63–0.72) and Eu–depletion type (Fig. 10l, δEu: 0.60–0.96; FeO^T/(FeO^T+MgO): 0.56–0.71). The An–Ab–Or diagram shows that the Eu–enrichment type has the characteristics of trondhjemite–granodiorite–tonalite, and the Eu–depletion type has granodiorite– tonalite characteristics (Fig. 7). Compering with other Eu–depletion type charnockites, Eu–enrichment type samples are relatively depleted in FeO^T, MgO, K_2O, Na_2O, CaO, P_2O_5, TiO_2, Nb, and enriched in Al_2O_3, Ba, Rb (Fig. 8). Eu –enrichment type sample has the characteristic of the Calclic series, Eu–depletion type sample has Calclic to Calclic–Alkline characteristics. The content of total REE

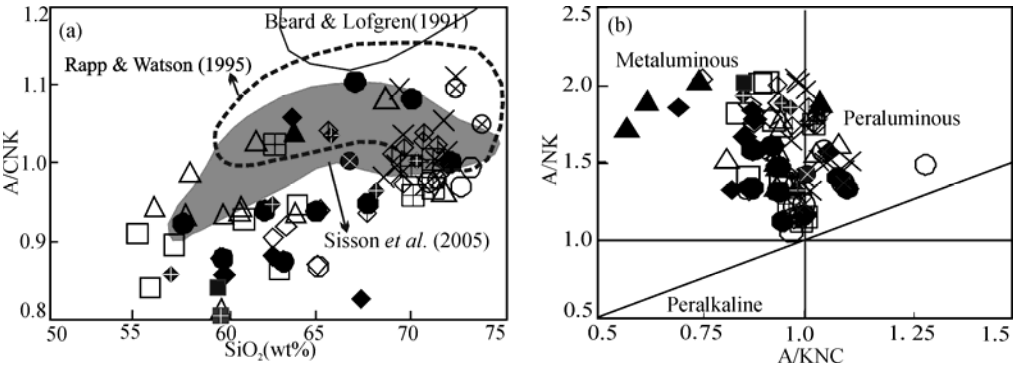

Fig. 11. The diagram of the SiO_2 vs. A/KNC (after Rajesh et al., 2011) (a) and the A/KNC vs. A/NK (Frost et al., 2001) (b) in Eu–enrichment type and Eu–depletion type charnockite samples from the north margin from NCC{The legend is the same as Fig. 8}.

is relatively high in samples with low Eu/Eu* values (Fig. 10l, Eu–enrichment type ΣREE: 40.68–56.23 ppm; Eu–depletion type ΣREE: 75.24–220.29 ppm), and all of them has the characteristic of HREE– depletion obviously. The total trace elements content of Eu–enrichment and Eu–depletion type sample is very similarity, all of them enriched in LILEs (eg. K, Rb, Ba), depleted in HFSEs (eg. Nb, Ta, Nd, P and Ti). Specially, the Eu–enrichment type sample (Fig. 10l) enriched in HPEs (eg. Th), more depleted in partial LILEs (eg. Rb and Ba) and HFSEs (eg. Ta, P, Nb and Ti). The ratio of A/CNK is 0.74–1.04, with the characteristic of metaluminous to weak peraluminium (Fig. 11b).

6 Discussions

6.1 Petrogenesis and sources rock

Shi et al. (2019b) studies shown that JN Charnockite has a typical characteristic of anatectic structure, such as the exists universally of sieve texture in garnets that the mineral assemblages of the peak stage of granulite facies metamorphism (Pl+Cpx+Hb+Qtz) are retained. Ma et al. (2013a), Zhang et al. (2014), Shi et al. (2019a) refer to XWLBL Charnockite has the typical characteristics of meta–anatectic mineral. And the similarity typical anatectic structure in SHY Charnockite, with the granulite facies metamorphism mineral assemblages of Pl+Hy+Di+Hb+Qtz (Xu et al., 2015). In this study, the characteristic of anatectic charnockites are closely symbiosis with the basic–felsic granulite (Wulashan–Xinghe group) in space, and the leucosome felsic zone and dark granulite xenoliths development, indicating the anatectic melting occur migration and differentiation (Fig. 2a, 2c, 2e, 2g, 2i, 2k). In general, the hypersthene in anatectic characteristics charnockite (Magnesian–charnockite) has a xenomorphic structure and irregular in shape, associating with plagioclase accumulation. The characteristics of plagioclase and quartz peritectic in the crystal show that hypersthene is a typical metamorphism genetic. The hypersthene in magmatic genetic characteristics charnockite (Ferroan–charnockite) has the characteristics of tabular structure, and it does not have the sieve texture, with a typical magmatic genetic characteristic. We noticed that the typical granulite facies metamorphism mineral assemblages (Pl+Cpx+Hb+Qtz) which has the characteristics of typicaly erosion structures, with a harbour–like structure and some of them have residual amphibole and biotite in anatectic charnockites (SHY Eu–enrichment type Charnockite, CKS Charnockite, LYS Charnockite, BQG Charnockite, XWLBL Charnockite, JN Eu–enrichment type Charnockite, Hereinafter refered to as ‘anatectic charnockites’), and all of these phenomena indicate the formation of metamorphism–anatectic charnockites (Figs. 2b, 2d, 2f, 2h, 2j, 2l). The residual mineral phases of pyroxene and garnet have generally sieve texture (Fig. 2d, 2f, 2h, 2l), with melting corrosion structure of Pl+Hb+Qtz mineral assemblages, and raising to a mineral assemblages of granulite facies metamorphism of the stage of prograde metamorphism (Lu et al., 1992, 1993; Shi et al., 2019b). Previously study of traditional calculation of temperature and pressure may suggest that isothermal decompression after peak metamorphism was intimately related to the formation of anatectic charnockites (Shi et al., 2018; Shi et al., 2019a), in which consistent with the anatectic characteristics charnockites in this paper.

The coexistence of Eu–enrichment and Eu–depletion type charnockites are prossesing a partition curve of Eu–enrichment type considered to be a typical feature of NCC anatectic granite, considered as a typical anatectic feature (Song et al., 2005; Ma et al., 2015; Shi et al., 2018), related to the redistribution of elements in the process of anatexis. Eu anomaly become the most obviously difference to the charnockites in southern India (Stuckless et al., 1989). The partition curve of Eu–enriched and Eu–depleted of the anatectic characteristic granite in the field (SHY Eu–enrichment type Ccharnockite, BQG Charnockite, LYS Charnockite, CKS Charnockite, XWLBL Charnockite, JN Eu–enrichment type Charnockite), relatively enriched in LILEs (eg. K, Rb, Ba). It is also suggested that they are readily partition into the meltting and may be a small amount of fluid during the anatexis, and more depleted in HFSEs. These differences compositions of the trace–element may be reflected by the redistribution of chemical components during the anatexis. The characteristics of radiogenic elements (eg. Th and U) depletion can further support to an anatectic origin.

Previously experiment study indicated that the partial melting of continental crustal material, with the refractory residual REE enriched mineral of zircon and apatite which reduction of REE content in anatectic products (Gordon et al., 2013). The geochemical characteristics of anatectic charnockites are obviously depleted in the content of "P" that mainly related to the mineral of apatite. Hidaka et al. (2002) study indicated that the Eu anomaly is closely related to the melanocratic mineral of plagioclase, hypersthene and garnet, raisesing a explanation for Eu–enrichment and Eu–depletion type anatectic charnockites. Comparing with Eu–enrichment type sample, Eu–depletion type sample has a relatively lower content of CaO and CaO+Na_2O, however, the content of FeO^T, MgO, Nb, Ta, Zr, Hf, U, Th relatively higher (Figs. 8, 10), and a lower content of Sr (Table 1). All the characteristic of Eu–depletion samples has a higher content of melanocratic mineral and a lower content of plagioclase. The total amount of REE in Eu–enrichment samples is generally lower, and in some samples even 4–6 times lower than that in Eu–depletion samples (Table 1). We consider that the higher content of plagioclase and lower content of melanocratic mineral in NCC charnockites that further explained the primary separation of residual minerals of pyroxene (One of the mainly restricting factors of REE content of continental crust rocks) and new leucosome during the crystallization process. The REE characteristics of charnockites may be influenced by the refractory residual minerals such as zircon and apatite.

We can observed a obviously depletion characteristics of HREE relative to LREE in the charnockite samples [$(La/Yb)_N$=4.0–77.4] possible indicated that the presence of residual garnet in the source region of these charnockites since HREE can be strongly fractionated into garnet in consisten with the study by Johnson (1998). However, there are also possessed a high ratio of the $(La/Yb)_N$ from the sources rocks. Nagasawa (1970) study raised to the zircon may be cause to a strongly partition HREE over LREE, therefore, the fractionation of zircon may also cause to the HREE–depletion that we observed in this paper charnockites. And the characteristics of slight Zr depletion samples indicated that the zircon as a fractionating phase only plays a minor importance part of the charnockites in this paper. However, the feature of Zr enrichment in these charnockite samples may raise to accumulation of the zircon during its magmatic crystallization history. In this paper, we considered that the combined action of the residues of residual minerals such as apatite may lead to a sharp decrease in the total REE content of charnockite. In general, the geochemical characteristics of the anatectic charnockites in this region are as follows: the distribution of major and trace elements is extremely uneven, with the depletion of LILES (eg. Cs) and HFSEs (eg. U and Th) obviously, relatively more enriched in Sr and depleted in HFSEs (eg. Nb, Ta, P and Ti). Prossesing a unique REE partition curve of Eu enrichment and Eu depletion that not only the mainly particular characteristics of charnockites in this region. And the anatectic granite shows a similar characteristic in the Baotou and Jining area (Song et al., 2005; Ma et al., 2015; Shi et al., 2018). We confirmed that some variability and inheritance of geochemical characteristics of the charnockits, the former may be related to the subsequent convergence and migration of anatectic melting and the latter may be related to the source rocks.

The various geochemical characteristics of charnockites can usually indicate the tectonic background of formation. Frost and Frost (2008) summarized the major geochemical characteristics of the formation of charnockites in different tectonic settings: ① Rift–related charnockite has the characteristics of ferroan alkali–calcic to alkalic metaluminous, as the component rocks of Anorthosite–Mangerite–Charnockite–Granite suite (Emslie, 1991). ② Delamination–related granites have the characteristics of small–volume, alkali–calcic to alkalic and magnesian plutons that connected with the delamination of thickened continental crust after a collision orogeny event. ③ Deeply crustal partial melting related granite has the characteristics of the upwelling of hot ferroan magma, the compositions of geochemistry and isotopic indicated the crustal component has been involved (Young et al., 1997; Battacharya and Sen, 2000; Kar, 2003; Percival et al., 2003). ④ Deeply eroded has the characteristics of alkali–calcic to alkalic and metaluminous granitoid chemistry plutons, indicating a deeply eroded magmatic arc tectonic settings. Ferroan–charnockite in the northern margin of NCC is different from the Qianxi ~1.95 Ga Ferroan–charnockite in Hebei Province ($FeO^T/(FeO^T+MgO)$: 0.9–1.0, #Mg: 6–28) in this paper (Yang et al., 2014), Jining and Shanheyuan Ferroan–charnockite (JN Eu–depletion type and SHY Eu–depletion type Charnockites, Hereinafter refered to as 'Ferroan–charnockite') has weak ferroan characteristics (Table 1, $FeO^T/(FeO^T+MgO)$: 0.84–0.96, #Mg: 7–37) Eu–enrichment type sample has the characteristic of Calclic to Calclic–Alkline, Eu–depletion type has the characteristic of Calclic–Alkline to Alkline–Calclic. Magnesian–charnockite (SHY and JN Eu–enrichment type Charnockite, CKS Charnockite, BQG Charnockite, LYS Charnockite, XWLBL Charnockite, hereinafter referred to as 'Magnesian–charnockite') are classified into Eu–enrichment type (Calclic to Calclic–Alkline characteristics) and Eu depletion type (Alkline–Calclic to Alkline characteristics). Above mentioned charnockites are consistent with the evolution of island arc magma along a calc–alkaline trend (Fig. 12b, Magnesian and Ferroan charnockite characteristic, Calclic to Calclic–Alkline to Alkline), and all of them inconsistent with the Rift–related and Delamination–related granite. Comparing with the geochemistry characteristic of closely spatially granulite (Fig. 1, 2), and the characteristic of crustal sources of Nb–depletion (Fig. 10), with the typical characteristic of plutonic rock. We consider that charnockites are related to the partial melting of lower crustal and island arc magma plutonic rock, they are associated with the granulite facies metamorphic. In the field, we can see the Eu–enrichment type charnockite often has gneissic texture which similarity to the characteristic of TTG gneisses, and some of them may be related to crust-mantle interaction (Rajesh, 2007; Frost and Frost., 2008). However, the most Eu–depletion type is massive is related to the extensional background (Chacko et al., 1992; Rajesh, 2012; Yang et al., 2014, except for late superimposed metamorphism), also has an island arc

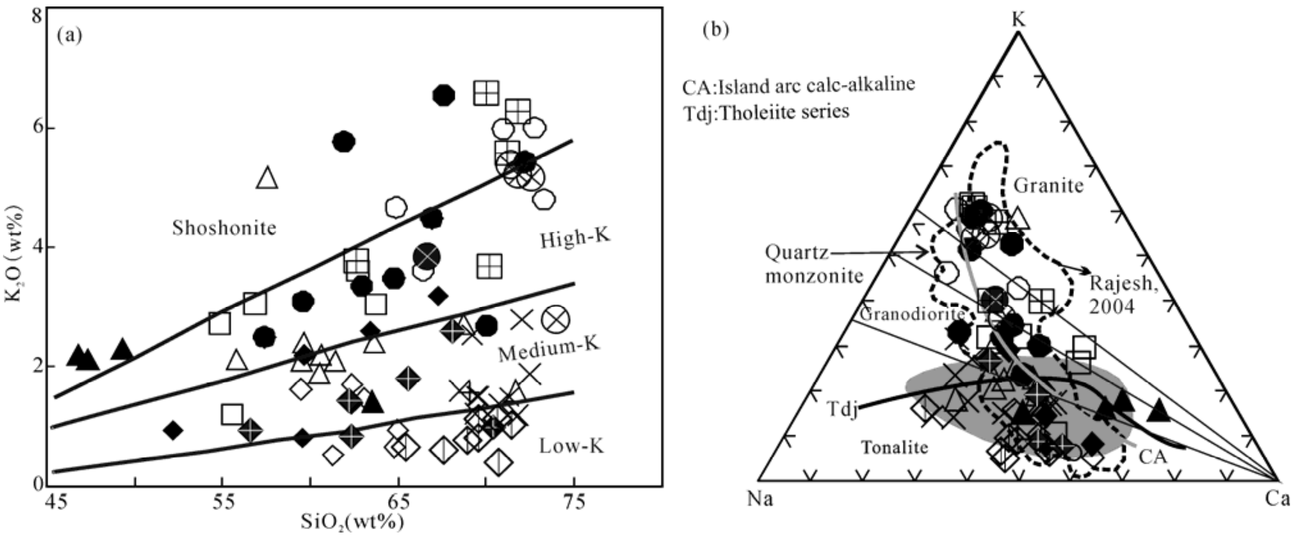

Fig. 12. The diagrams of the SiO_2 vs. K_2O (Peccerillo and Taylor, 1976) (a) and the K vs. Na vs. Ca (Barker and Arth, 1976) (b) in Eu–enrichment type and Eu–depletion type charnockite samples from the north margin from NCC{The legend is the same as Fig. 8}.

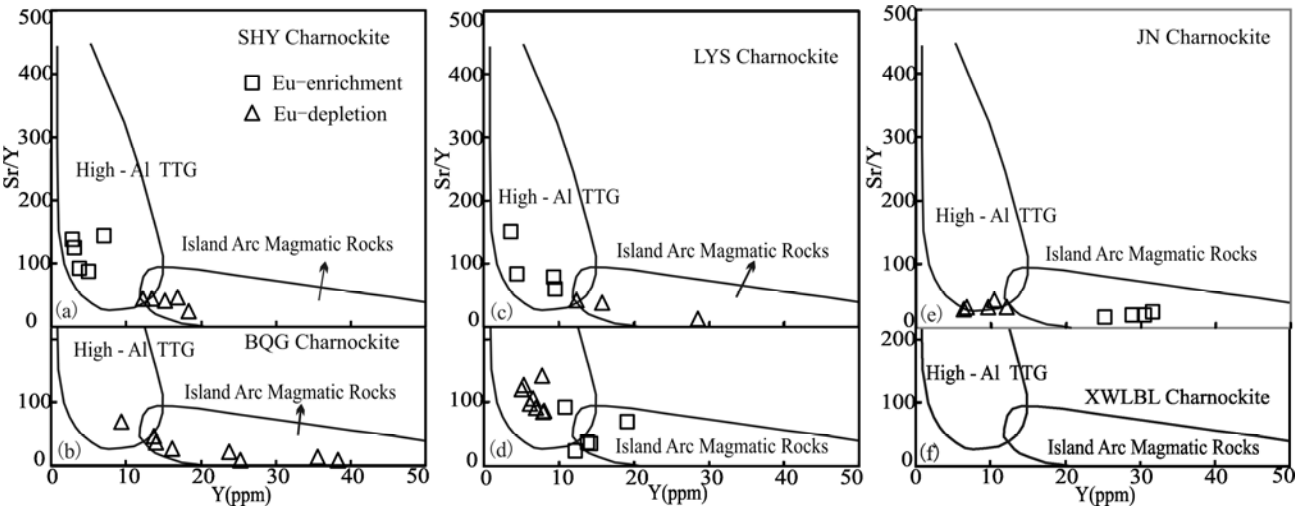

Fig. 13. The diagrams of the Y vs. Sr/Y in Eu–enrichment type and Eu–depletion type charnockite samples from the north margin from NCC (Drummond and Defant.,1990).

magmatic magma characteristic (Fig. 13).

The southern India and other different parts of the world obtained the compilations of geochemical data from charnockites, indicating the mostly Magnesian–charnockite belong to tonalitic rocks (trondhjemitic rocks are more likely to magnesian, but occurrences rarely related to the tonalitie rocks), whereas the Ferroan–charnockites are more likely to granodioritic–granitic rocks (Rajesh, 2007). In general, Frost and Frost (2008) study refer to the Ferroan–charnockites are more likely occured in an extensional tectonic enviorment whereas Magnesian–charnockites more likely formed in a magmatic arc setting (Rajesh, 2007). Similar to the southern India charnockites, JN Eu–depletion type and SHY Eu–depletion type Charnockites (Ferroan–charnockite) mainly belong to monzogranite–granite characteristics, however, anatectic charnockites (Magnesian–charnockite) has the granodiorite–tonalite characteristics. And all of them has the trend of calc–alkaline magma evolution of island arc (Fig. 12b).

Charnockite is characterized by high Ba–Sr in this paper. Previously study raised to almostly all of the genetic mechanisms proposed for the high Ba–Sr charnockite formation require the lithospheric mantle material addition, such as (1) Qian et al., (2003) studies consider that high Ba–Sr granite derived from the melting of subcontinential lithospheric mantle; (2) Fowler (2001) refer to the Ba–Sr granite may be a production of crystal fractionation of associated shoshonitic magma derived from an enriched lithospheric mantle; (3) Shi et al. (2018, 2019a) studies indicated that high Ba–Sr anatectic granite related to the underplating of Sr– and Ba–rich mafic magma; (4) Ye et al. (2008) raise a point of view about high Ba–Sr granite is the products of partial melting of lower crust with a minor involvement of enriched mantle derived magma. Qian et al. (2003) refer to the melt of continental lithospheric mantle generally forms potassic magmas ($K_2O+Na_2O>5$ wt%, $TiO_2<1.3$ wt%, Al_2O_3: 14–

19 wt%), however, the charnockite has the trend of calc–alkaline magma evolution of island arc in this paper (Fig. 12b), with a small part of samples have the characteristics of potassic. It is considered that more alkaline ($K_2O+Na_2O>5$ wt%) and enriched in K_2O ($K_2O/Na_2O>0.7$) of crystal fractionation of shoshonitic magma generates melt, which is inconsistent with the K_2O content of the charnockites in this paper. The depleted in Nb and Ti characteristic, which together are consistent with a continental crustal origin distinct from single mantle–derived magma. However, the difference of the degree of Nb–depletion raised to the problem of the charnockite formation. The isotope geochemistry of XWLBL High–Ba and Sr charnockite indicated that consistent with an underplating of Sr– and Ba–riched mafic magma during the process of the anatexis (Ma et al., 2013a; Zhang et al., 2014; Shi et al., 2018). Similar to the geochemistry of XWLBL Charnockite, anatectic charnockites transitional to source rocks in spatial (Shi et al., 2018, 2019a), and has a characteristic of High–Mg content (Table1, #Mg>45), in which indicated more mafic sources than basalt. Combined with the low content of Nb (<10ppm) elements and the value of εHf>0 in most samples (In Table 2), mainly derived from juvenile crustal material and the addition of high Sr–Ba ingredient from the mantle. Therefore, the single source of mantle–derived magma is not credible. However, high Ba–Sr and Eu–depletion type charnockite studies of Jining area raise to petrogenesis of crystal fractionation of associated shoshonitic magma, while the Eu–enrichment type charnockite addition of high Sr–Ba ingredient from the mantle during the anatexis (Shi et al., 2019a). The geochemistry of SHY Eu–depletion Charnockite is similar to Jining Eu–depletion Charnockite, the values of εHf is –9.74–3.56 (in Table 2, Liu et al., 2017), and all of them has the low Mg content characteristic ($Mg^{\#}<45$), indicating the more basalt sources than mafic. At the same time, the content of Nb relatively higher (Nb>15ppm) than anatectic charnockite (Average content of Nb:10 ppm) that raising to a few of crustal material sources, and the geochemistry characteristics of K, Na content is consistent with crystal fractionation of associated shoshonitic magma. However, the crystal fractionation usually with the Eu–depletion characteristic (Ye et al., 2008), similar to JN Eu–depletion charnockites, we consider that SHY Eu–depletion Charnockite has the original of crystal fractionation associated with shoshonitic magma. Similar to the XWLBL charnockite, SHY Eu–enrichment type and JN Eu–enrichment type Charnockites are more likely related to the anatexis of the juvenile lower crustal.

For anatectic granite rocks, Drummond and Defant (l990) refers to the depleted in Y and HREE, with a higher ratio of Sr/Y and La/Yb posibility formation by hornblende, clinopyxene and garnet in residual phases after partial melting. All these characteristics are more similar to Eu–enrichment type anatectic charnockites, but the mafic granulite delamination occurring in lower crustal that the partial melting happened can formation the evolution of Eu–depletion anomaly characteristic (Gao et al., 1997; Gao et al.,1999). It is inconsistent with the Eu anomaly characteristic indicated that the source of anatectic charnockite is not only the mafic material in this paper. The digrama of SiO_2 vs. A/CNK consistent with the composition of the water–bearing melt at high temperature (Fig. 11a, Sisson et al., 2005), indicating the charnockites in this study area may be have a water–bearing basaltic source rock, and having the mixed composition characteristics of the experiment sample of Beard and Lofgren (1991), Rapp and Watson (1995) and Sisson et al. (2005).

Experimental petrology studies indicated that granitic magma can be formed from many common rocks under widely temperature and pressure conditions, in view of the different geochemical identification markers to discriminate the different components of protoliths (Rajesh and Santosh, 2004). The compositional difference of partial melts pro–from sources, such as greywackes, pelites, and amphibolites can be visualized (Fig. 15). It follows from figure 15 that the original melt of the NCC charnokitesss may be derived from a mafic pellite and amphibolitic source. Experimental studies raise to the partial melting of hydrous basalt can produce the low $Mg^{\#}$ magmas ($Mg^{\#}<45$), regardless of the pressure conditions (Rapp et al.,1991; Rapp and Watson, 1995), further supporting the Ferroan– charnockite original of crystal fractionation of associated shoshonitic magma that the more basaltic sources than mafic, and all of them has a amphibolite volcanic original rocks (Fig. 15). In anatectic charnockite, Eu–enrichment type samples of has the characteristics of high–Mg content ($Mg^{\#}>45$) that revealing the more mafic pellites sources than basalt (Rapp et al., 1991; Rapp and Watson 1995). However, Eu – depletion type has characteristics of amphibolite volcanic original rocks, and more likely a basaltic source

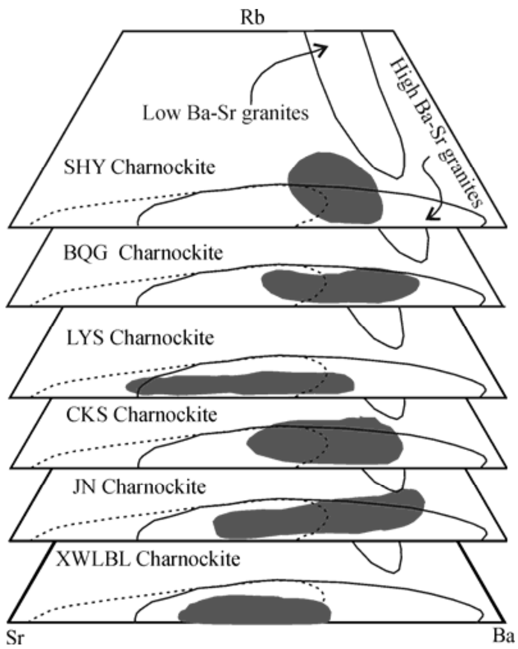

Fig.14. The diagram of the Rb vs. Sr vs. Ba in Eu–enrichment type and Eu–depletion type charnockite samples from the north margin from NCC after Rajesh and Santoshi (2004)

Table 2 zircon U–Pb age and Hf–Nd isotope statistics in North China Craton

Rock		Location	Age (Ma)	Metamorphic Age (Ma)	ε_{Hf}	T_{DM} (Ma)	Method	Data from
Metamorphic Complex	XWLBL Charnockite	E 110°42′00″ N 40°57′00″	2533±15	2490±11	2.3–5.5	2648–2779	LA–ICP–MS	Ma et al., 2013b
		E 110°42′00″ N 40°57′00″	2524±17	2498±3	1.4–4.9	2631–2749	LA–ICP–MS	Ma et al., 2013b
		E 110°55′12″ N 41°07′31″		2512±10	–1.4–2.3	2712–2782	LA–ICP–MS	Zhang et al., 2014
		E110°54′06′ N 41°03′12″	2525±8				SHRIMP	Jian et al., 2012
	LYS Charnockite	E 110°55'25″ N 41°04'19″	2548±24	2496 ± 36	–4.21–7.36	2649–2806	SHRIMP	Ma et al., 2013
		E 110°45'43″ N 40°55'47″		2506±9 2479±12	–1.6–8.09	2645–2880	SHRIMP	Dong et al., 2012b; Ma et al., 2013c
	JN Charnockite	E 118°56′49" N 41°01′08"		2469±9			SHRIMP	Shi et al., 2019
		E118°57′18" N 41°00′55"		2474±15			SHRIMP	Shi et al., 2019
		E112°35′26" N41°04′02"		2492±29			SHRIMP	Shi et al., 2019
	SHY Charnockite	E110°54′06′ N 41°03′12″		2484±7 2494±12	0.22–3.92	2608–2782	SHRIMP	Xu et al., 2015
		E110°18′06′ N 40°43′12″		2455±8	–9.74–3.56	2522–2642	SHRIMP	Liu et al., 2017
	BQG Charnockite	E110°18′06′ N 40°43′12″		2455±15 Ma	0.22–3.92	2602–2674	SHRIMP	Liu et al., 2017
	CKS Charnockite	E109°41′52′ N 40°41′56″		2484±6	3.7–7.0	2532–2658	SHRIMP	Ma et al., 2012
		E109°33′52′ N 40°56′56″		2484±6			Single Zircon	Wang et al., 2001
	GHY Charnockite	E114°25′06″ N 40°15′12″		2502±10 2512±12			LA–ICP–MS	Zhang et al., 2017
	GHY Hypersthene Tonalite	E114°25′16″ N 40°17′23″		2502±10 2512±12			LA–ICP–MS	Zhang et al., 2017
	Gneiss	E110°28′13′ N 40°39′16″		2459±7 2454±7	3.39–6.29	2564–2624	LA–ICP–MS	Liu et al., 2017
		E109°30′34′ N 40°41′27″		2432±29	–0.2–8.4	2015–2606	SHRIMP	Ma et al., 2012
		E109°38′29″ N 40°42′40″		2444±9	–4.9–7.4	2478–2656	SHRIMP	Ma et al., 2012
	Granulite	E109°40′37″ N 41°34′40″		2452±8			SHRIMP	Cai et al., 2012
		E 110°45'43″ N 40°55'47″	2545±10	2503±10	–2.30–6.49	2634–2757	SHRIMP	Dong et al., 2012a; Ma et al., 2013c
		E 110°34'12″ N 41°10'07″		2511±5			Camara	Zhang et al., 2005
		E 110°35'05″ N 40°57'59″		2512±16			LA–ICP–MS	Liu et al., 2016
		E 110°51'03″ N 41°05'24″	2544±5	2503±12			SHRIMP	Jian et al., 2012
Granitoid	Diorite	E 110°39'41″ N 41°17'23″		2503 ± 7	–0.66–4.44		SHRIMP	Ma et al., 2013
	sanukitoid	E 110°45'43″ N 40°57'28″	2523±7		1.5–6.3		LA–ICP–MS	Ma et al., 2013b
	TTG	E 110°06'14″ N 41°31'34″	2534±7				SHRIMP	Ren et al., 2010
	TTG	E 110°00'18″ N 41°18'20″	2515±6				SHRIMP	Jian et al, 2012
	Andesite	E 110°35' 50″ N 41°02' 02″	2510±7				SHRIMP	Jian et al, 2012b
	Basalt	E 110°34' 09″ N 41°02' 02″	2516±10				LA–ICP–MS	Chen et al., 2007
	High–Mg Andesit	E 110°35' 50″ N 41°02' 02	2533±5				SHRIMP	Jian et al., 2012
	Basalt	E 110°33' 58″ N 41°08' 59″	2562±14				Camerca	Liu et al., 2012

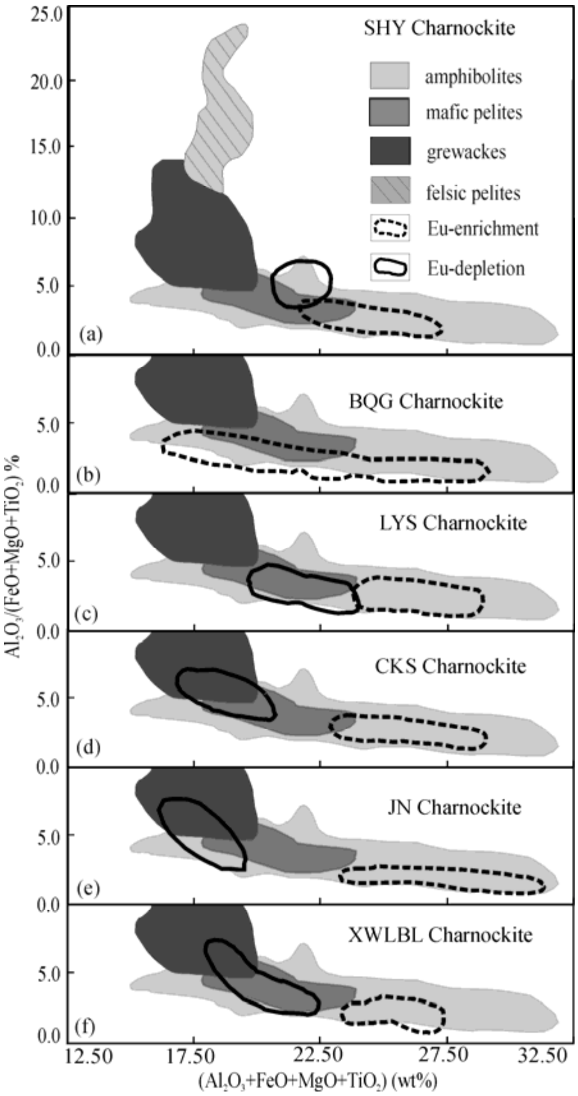

Fig. 15. The diagram of the $Al_2O_3/(FeO+MgO+TiO_2)$ vs. $Al_2O_3+FeO+MgO+TiO_2$ (wt%) in Eu enrichment type and Eu depletion type charnockite samples from the north margin from NCC Rejesh and Santosh (2004).

and mantle material addition.

The chemical compositions of charnockite samples from NCC seem to have an extensive compatibility with mafic pellites and basaltic source, especially the anatectic charnockite. Frost and Frost (2008) studies considered that comparing with the basalt, ferrodiorit is more likely to be the protolith of charnockites formed by crustal melting, because of its melting point is lower than basalt, and iron ferro–basalts more exists in extensional environments. Experimental petrological study shows that mainly composition of ferrodioritic source compositions melts is monzonite (Scoates et al., 1996), while the opx–bearing monzonites have not been found among the NCC charnockites considered in this study (Le Maitre., 2002). The coexistence of Eu–enrichment and Eu–depletion geochemical characteristics are more similar to South India intermediate–felsic charnockite (Chacko et al., 1992; Rajesh, 2012). Therefore, we considered that the anatectic charnockite may be has a part of basaltic sources. Eu anomaly of anatectic charnockite is especially prominent and becomes a typical character of most of the anatectic rocks. In addition to the mineralogical explanation above, we are trying to make a further studiy from the sources. Strongly peraluminous melts (A/CNK>1.1), like Southern India Nilgiri garnetiferous charnockites, all of them are commonly taken to have formed by a sedimentary source. However, the anatectic charnokites in this paper has a metaluminous to week peraluminous characteristics (A/CNK<1.1), and the use of a different set of geochemical discrimination factors does not rule out the igneous affinity of the source rock of NCC charnokites (Fig. 16). Furthermore, igneous enclaves present within both Eu–enrichment and Eu–depletion type anatectic charnokites from the NCC indicates that more mafic magmas and/or other igneous sources may have been involved in the origin of both types of magma.

Previously geochemical views indicated that metafily wackes, felix orthogneises and amphibolites possibly become source to produce the peraluminous charnockites. There are also tending to produce only small quantities of strongly peraluminous melting (A/CNK >1.3) shown by Pelitic sediments melting experiments, however, they are not suggesting as the mainly source for the NCC anatectic

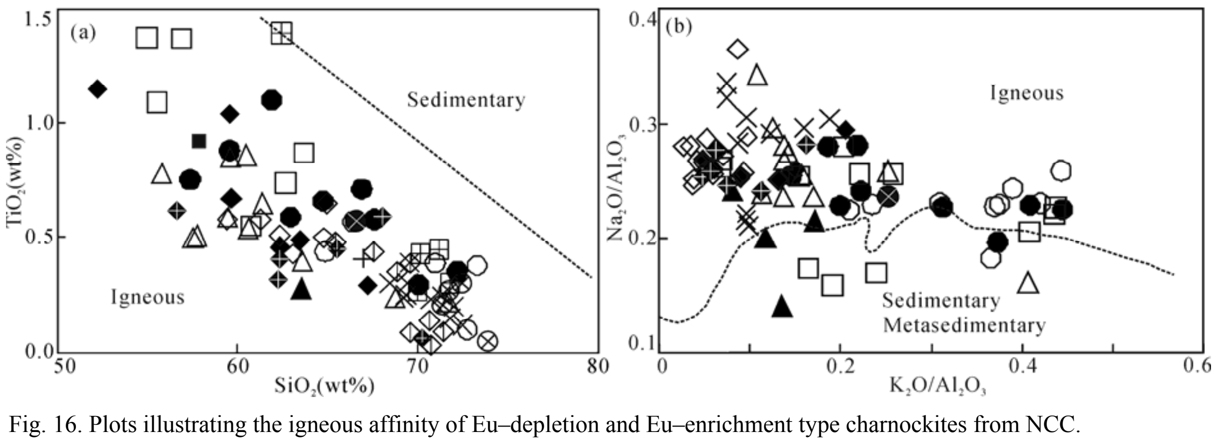

Fig. 16. Plots illustrating the igneous affinity of Eu–depletion and Eu–enrichment type charnockites from NCC.
The igneous–sedimentary dividing lines in the TiO_2 vs. SiO_2 plot and Na_2O/Al_2O_3 vs. K_2O/Al_2O_3 plot are from Tarney. (1976) and Barrels and MacKenzie. (1971). The legend is the same as Fig. 11.

charnockites melts with lower A/CNK values (usually<1.1). Futher more, previous study shown that the K_2O/Na_2O ratio of a pelitic source melting is much higher (Montel and Vielzeuf., 1997, average of K_2O/Na_2O ratio: 4–24) than the ratio in the least evolved samples of NCC Eu riched and Eu depleted type anatectic charnockite which the Eu–enrichment type (K_2O/Na_2O: 0.94–1.03) higher than Eu–depletion type (K_2O/Na_2O: 0.83–0.97) in Table 1. We can see the Eu–enrichment type anatectic charnockites have more mafic pelites sources, however, Eu–depletion type has the more sources of amphibolitic rocks sources in Figure 15. The more feldspar and quartz riched metagreywackes and orthogneisses are potentially fertile sources and could be produced a relatively large volumes of moderately peraluminous melts (Fig. 15), the production of differences composition of partial melts derived from greywackes, pelites and amphibolites can be found visualized. And we can see in the Figure 15, the original melting of the anatectic charnockites may be derived from an amphibolitic rocks and mafic pelites sources, and the Eu anomaly characteristic may be related to the content of amphibolitic rocks and mafic pelites, also influenced by the underplating of Sr and Ba–riched mafic magma. The similar affinity of the parent rocks for the anatectic charnockites from the NCC and the India South high Ba–Sr charnockites massifs (Rajesh, 2004) are substantiated by their similarity to high Ba–Sr granitoids with low K_2O/Na_2O ratios (Fig. 12b) and other elemental characteristics (Supplementary Table1, high content of Sr, Ba and LREE, the low Y and HREE, elevated La/Yb) that are typical of adakites and Archaean TTG suites (Fig. 12b, Martin,1986; Drummond and Defant,1990). This character is different from those of charnockites fractional crystallization product of shoshonitic magma, like those of the SHY and JN Eu–depleted massif, which show a similarity to high Ba–Sr granitoids with low Ba and high Y ratios (Figs. 10, 12).

The feature of Nb depletion has considered to be a typical crustal sources rock. All the geochemical discussion above, considered that Eu–enrichment samples have a mafic pellites sources and Eu–depletion samples have a protolith of basaltic rock for anatectic charnockites. With a widely variety of pressures, the experiments of amphibolite dehydration melting generate a TTGs magmas conducted at 750–1000℃ (Rushmer.,1991; Beard and Lofgren, 1991; Patiño Douce and Beard,1995), which has a similar or indistinguishable composition of charnockites studied in this study. The degree of partial melting and residual mineral assemblages are controlled by the heat ultimately (Rajesh et al., 2004). Dehydration melting experiments showed that hornblende is absolutely consumed at the temperature of 925–1000℃, leaving a granulitic residue mineral association of orthopyroxene, clinopyroxene, plagioclase and Fe–Ti oxides with garnet at higher pressures (Rushmer,1991). When the temperatures of the melting is higher, the remaining minerals partially consumed (Rajesh et al., 2004). Although the latter stage of partial melting is mainly the plagioclase, and residual mineral assemblage remains is not changed under a condition of the isobaric temperature increase. Most experiment of metabasaltic sources dehydration melts are strongly peraluminous (Patiño Douce,1997), however, dehydration melts will be produced from metabasaltic sources at a very high temperature of partial melting (>1000℃), the melting start to have a metaluminous characteristic (Rapp et al.,1991). The characteristic of low contents of K_2O, a relatively high contents of Na_2O and the values of $Mg^{\#}$, whatever the degree of partial melting, making the meta–basaltic rock suitable source rocks for anatectic charnockites.

Experiments of dehydration melting by using the basaltic starting materials yielded melts is similar to the NCC (Fig. 17, Beard and Lofgren's., 1991), and the experiments of Springer and Seck (1997) studies also using basaltic starting material showed that with rising temperatures at constant CO_2 content, and it is also similar to the southern India intermediate charnockites. The experiments of Kaszuba and Wendlandt (2000) indicated that with increaseing the content of CO_2 at the constant–temperature, similar to the most evolvement of anatectic charnockites that the melts become richer in the content of normative orthoclase. Besides, the CO_2 riched melt is more likely to enrich in K, Ba, and Zr (Eggler et al., 1987) that CO_2 riched fluid inclusions have referred from some charnockite (Srikantappa, 1996; Santosh et al., 2003; Rajesh, 2004), and it is similar to the characteristic of anatectic charnockites from North China (Fig. 8). Same as the southern India charnockites, lacking of K–depletion and extreme Rb–depletion in some of the high tempreture–pressure Archaean charnockites from NCC may also mirror a fluid phase existence with a relatively higher ratios of the CO_2/H_2O (Weaver et al., 1980; Condie and Allen, 1984).

In the case of Eu–depletion type and Eu–enrichment type anatectic charnockites massifs and granulite showing close spatial association (and possibly temporal) from NCC, the characteristics of their near continuous variations in geochemistry compositions probably point

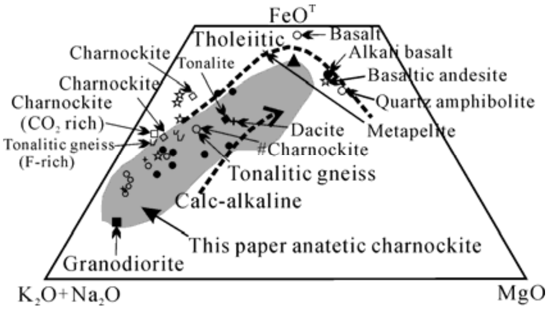

Fig. 17. AFM (wt%) plot of the NCC anatetic charnockites and experimental data on compositions of partial melts derived from a variety of crustal and mantle rocks by water–under saturated melting.

The different rocks are from: Dacite (Beard and Lofgren,1991); Basalt (Beard and Lofgren,1991); Basaltic andesit (Beard and Lofgren,1991); Tonalitic gneiss (Skjerlie et al.,1993); Metapelite (Skjerlie et al., 1993); Tonalitic gneiss (F–rich) (Skjerlie et al., 1993); Charnockite (Beard and Lofgren.,1991); Charnockite (CO_2–rich) (Beard and Lofgren.,1991; Quartz amphibolite (Patiño Douce and Beard, 1995); Tonalite (Patiño Douce, 1997); Granodiorite (Patiño Douce, 1997); #Charnockite (Litvinovsky et al., 2000); Alkali basalt (Kaszuba and Wendlandt, 2000). The respective compositions of the starting material (indicated by arrow) and the product(s) of water–under saturated melting of some of these rocks are shown (by similar symbols).

out a genetic relationship between them (Shi et al., 2018; Shi et al., 2019a). If these two types of charnockites were distinguished from the similar parent magmas, the Eu–depletion charnockites may presumably represent a higher degree of separation and crystallization. For Eu–depletion charnockites, the absence or lower Eu anomalies may not develope many fractionation requirements for most of the charnockite formation (Rajesh, 2004). The constant ratios of the trace elements (Ce/Zr, Zr/Nb and Rb/Zr) is often considered to be the dominant process in the evolution of specific suites (Wilson, 1989). Obviously, the crustal melting and contamination are unlikely occurred, in the event of the ratio of trace elements remains in a suite. For the NCC charnockites, the above-mentioned characteristics of trace element ratios vary in both Eu–depletion and Eu–enrichment type charnockites. The separation and crystallization model can be argued against by some bimodality of the charnockite (eg. Pallavaram massif, with basic membere). So, the separation and crystallization might not be responsible for contrasts among Eu–depletion and Eu–enrichment type anatectic charnockites of the same rocks. For example, this would explain the Eu–depletion and Eu–enrichment characteristics and raise in the abundances of REE that correlate with the increasing of the content of the SiO_2 in some charnockites. Such comparison may influence by the distrinct degree of melting with lower degree melting point having a higher content of the SiO_2 and HREE, and characterized by the upwarping of the tail of the distribution curve of HREE. It is possible to explain the spatial association of Eu–enrichment and Eu–depletion anatectic type charnockites by a two–stage model, assuming an original lower degree of the partial melting and subsequent crystallization fractionation. We cannot get rid of the origin of fractional rather than batch melting for the formation of those charnockites, having the REE patterns with a characteristics of slightly positive Eu anomaly. The model indicated that the different melting ratio of the mafic pellites and basalts in the anatectic charnockites that the formation of mineral composition and content are different, and forming the unique Eu anomaly characteristics in the anatectic charnockites

6.2 Tectonic significance

Geochemical characteristics and the core–mantle–rim structure of zircon in charnockites further constrain metamorphic anatexis. Extensive U–Pb zircon geochronology studies have assessed the morphology, internal structure, and Th/U ratio of zircon in various rocks (Rubatto et al., 1999; Rubatto, 2002; Hoskin and Schaltegger, 2003; Geisler et al., 2007; Wan et al., 2011; Zhao et al., 2015). Previously study obtained abundant achievements in the chronology of charnockites in the northern margin of the NCC. JN Charnockite and retrograded biotite–hornblende gneiss obtained anatectic ages of 2469±9 Ma – 2492±29 Ma (Shi et al., 2019c), occuring in the stage of prograde granulite facies metamorphism, in which the formation of charnockite is closely related to ~2.5 Ga granulite facies metamorphism in the northern margin of NCC. Ma et al. (2013a) and Zhang et al. (2014) study shown that the XWLBL charnockite is the anatectic product of basic granulite, and obtained crystallization age of remelted magma at 2511±12 Ma–2512±10 Ma and 2490±14 Ma–2490±5 Ma. LYS Charnockite obtained an anatectic ages of 2478±12 Ma–2498±22 Ma, indicating a stage of prograde ~2.5 Ga isothermal decompression after peak metamorphism granulite facies (Dong et al., 2012a; Liu et al., 2017; Shi et al., 2019a). Xu et al. (2013) study for SHY Eu–depletion type Magnesian–charnockite obtained diagenetic ages of 2484±7 Ma–2494±12 Ma, Liu et al. (2017) obtained magmatic crystallization age of 2455±15 Ma from SHY Eu–enrichment type Ferroan–charnockite. GHY Charnockite obtained a magmatic crystallization zircon age of 2502±10 Ma–2512±12 Ma and a metamaphism zircon ages of 2484±36 Ma in GHY Hy–Tonalites (Zhang et al., 2017). Previously study indicated that Yinshan Block was affected by magmatism event at ~2.5 Ga (Table 2), and the Archean U–Pb zircon ages obtained from a wide range of high–grade metamaphism rocks. Guyang complex composed of the Meta–dacites (2516–2500 Ma, Chen, 2007), diorites and granitoids (2556–2520 Ma, Jian et al., 2012) and sanukitoid high–grade metamorphism rock (2523–2465 Ma, Ma et al., 2013b); Meta–gabbro and charnockites suites of XWLBL Complex obtained the ages of 2540–2500 Ma (Zhang et al., 2014); Orthopyroxene–bearing TTG gneisses also obtained the ages of 2545–2507 Ma in Wuchuan Complex (Dong et al., 2012b); Meta–sandstones obtained the ages of 2690–2450 Ma from the Huade Group (Liu et al., 2012); Orthogneisses from the Hongqiyingzi Group obtained the ages of 2535–2484 Ma and Sandstones from the Zhaertai Group obtained the ages of ~2500 Ma (Li et al., 2007). A set of common Komatite–Greenschist–TTG–Metamorphic gabbro–charnockite in the process of subduction–collision–extension evolution has been identified in the northern Guyang–Xiashihao–Wuchuan (Ma et al., 2013a; Ma et al., 2013b; Ma et al., 2016), and it is generally believed that the subduction and collision tectonic evolution of the oceanic crust took place from north to south in Wuchuan–Xiwulanbulang–Guyang area. The Archean basement of Shiguai (Wan et al., 2009, 2013a, 2013b, 2015; Cai et al., 2014; Xu et al., 2015)–Daqingshan (Wan et al., 2013a; Xu et al., 2015; Ma et al., 2015; Liu et al., 2012; Liu et al., 2017)–Wulashan (Cai et al., 2014)–Jining (Shi et al., 2018, 2019a)–Siziwangqi (Chen et al., 2017)–Gehuyao (Zhang et al., 2017) obtained isotope chronology metamaphic ages of ~2.5 Ga and ~2.45 Ga (Fig. 18). The ocean crust subduction collision orogenic event occurred in Yinshan block to ~2.5 Ga in NCC (Bai et al., 2015; Yang et al., 2016), and detail of subduction–collision–extension of the current orogenic event (Ma et al., 2013a; Ma et al., 2013b; Ma et al., 2013c; Ma et al., 2016). Island arc environment after subduction of oceanic crust at 2.52–2.49 Ga, with a large number of TTG and diorites, accompanied by a large number of charnockites associated with island arcs. During the 2.47–2.44 Ga, the ocean crustal closure and collisional orogeny development, with the mantle–derived magma underplating in extensional environment (Xu et al., 2013; Ma et al., 2013c; Nancy Chen et al., 2017; Zhang et al., 2017; Shi et al., 2018; Shi et al., 2019a).

Rajesh and Santosh (2004) and Rajesh (2012) studies

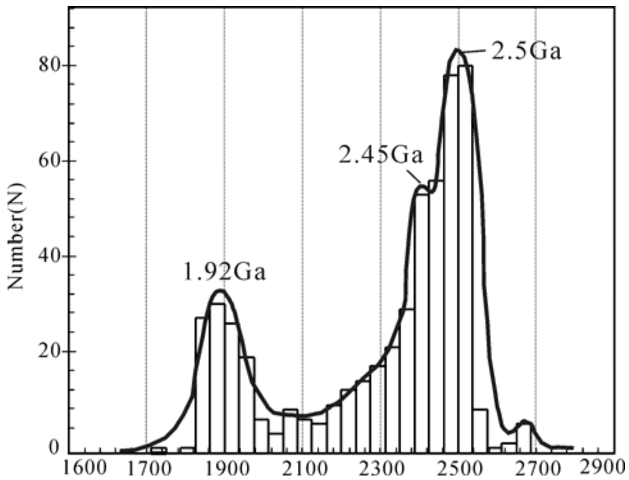

Fig. 18. Charnockites from Northern margin of NCC in terms of Age histogram diagram.

Data from: Li et al, 2011; Guo et al, 2012; Jian et al., 2012; Xu et al., 2013; Ma et al., 2013a; Ma et al., 2013b; Ma et al., 2013c; Liu et al., 2013; Cai et al., 2014; Zhang et al., 2014; Bai et al., 2015; Xu et al., 2015; Ma et al., 2016; Yang et al., 2016; Geng et al., 2016; Chen et al., 2017; Zhang et al., 2017; Liu et al., 2017; Shi et al., 2018; Shi et al., 2019c.

have shown that anatexis can occur in various tectonic settings, mainly in continental arcs and collision zones. It reflects the change of temperature and pressure conditions, with a concomitant phenomenon of high–grade metamorphism. These studies suggest that charnockite is a key to understand the lower crustal processes, discussing the petrogenesis and tectonic environment during its formation, geological significance to elucidate the growth and tectonic evolution of the early crust (Janardhan et al., 1982; Santosh and Yoshida, 1992; Frost et al., 2000; Kar et al., 2003; Rajesh, 2012; Rajesh and Santosh, 2012; Yang et al., 2014; Zhang et al., 2014). Geochemical studies suggest that the Ferroan–charnockite may be formed in extensional tectonic environment and the Magnesian–charnockite may be formed in magmatic arc environment (Frost and Frost 2008; Rajesh and Santosh, 2012; Rajesh, 2012). Peng et al. (2012) raised to a dominant origin from in situ melting of metamorphic sediments for the paleoproterozoic charnockites from the NCC, in which cannot suit to this situation. Lacking of the obviously sedimentary sequences in the Yinshan Block of NCC during the Neoarchean, and the geochemistry elemental inconsistency inconsiste with the production of the sediment melts and the metaluminous characteristics of the anatectic charnockites (Table 1), with the contrast of evolved isotopic geochemistry compositions between the juvenile crustal formation charnockites and meta–volcanic rocks (Table 2). JN Eu–depletion type and SHY Eu–depletion type Charnockite has the characteristics of Ferroan–charnockite (Fig. 6), while the anatectic charnockites has the feature of Magnesian–charnockite (Fig. 6). Frost (2008) study summarized the genetic background model for Indian charnockite, for fearron charnokitess, the heat and fluids released from mafic magma that has ponded at the base of the crust have produced granulite metamorphism in the lower crust under an extensional tecnotic environment. However, there are also an characteristic of arc environments for magnesian charnokitess which melting of the juvenile lower crust by the mantle magma underplating. Rajesh (2012) raised the South India charnockites related to the mantle basaltic magma underplating, with the converge of alkaline characteristics mafic magmas, and the charnockite formed be the partial melting of mafic lower crust. Upwelling of the basaltic magma with low water content might occur to dehydration melting of the lower crust formation the charnockite. In summary, combining with the understanding of the genetic model of Magnesian–Ferroan –charnockite in southern India (Frost et al., 2001) and the results on previous isotopic geochronology and geochemistry research, we consider that Late Neoarchean charnockites in the northern margin of the NCC, mainly related to the regional tectonic events of ~2.5 Ga and ~2.45 Ga (Fig. 18).

In this paper, the formation of anatectic (Magnesian) charnockite is more likely related to the generally ~2.5 Ga subduction of the oceanic crust in the northern margin of the NCC. Comparing with the geochemistry and isotope chronology achievements, and the mantle–derived magma associated with the arc may have formed in the island–arc environment after the subduction of the oceanic crust, with the anatexis of the younger basaltic lower crustal and the mafic pellites magma by the upwelling of anatectic melts. The anatectic charnockites are closely associated with the intermediate–basic granulite in space and transitional gradually (Fig. 19a), forming of the difference of composition of melting, with the coexistence of Eu–enrichment and Eu–depletion type of REE characteristics (Fig. 19a). The formation of Ferroan–charnockite (SHY Eu–depletion and JN Eu–depletion type Charnockites) might be related to the ~2.45 Ga tectonic event of NCC. We refer to the crustal thinning and pressure reduction inluenced by the underplating of basaltic shoshonitic magma and the crystallization differentiation of the melting under the back–arc extension environment of collision orogeny, and the addition of crustal source materials plays an important role (Fig. 19b).

7 Conclusions

(1) The distribution of major and trace elements in charnockite is very uneven. Significant depletion in LILEs (eg. Cs, U, Th), enrichment in Sr, depletion in HFSEs (eg. Nb, Ta, P, Ti). With the coexistence of Eu enrichment and Eu depletion type of REE patterns. Eu–enrichment type samples is relatively high content of plagioclase and low content of the dark mineral. The relative decrease of total REE may be affected by the remnants minerals of refractory by zircon and apatite.

(2) The anatexis of the younger basaltic lower crustal sources and mafic pellites sources, formation the characteristics of anatectic Magnesian–charnockite in NCC, with the upwelling of mantle magma. The difference ratios of mafic pellites and basalts sources involved in anatectic melting, resulting in the coexistence characteristics of Eu enrichment and Eu depletion REE patterns. Ferroan–charnockite is the product of the upwelling of mantle–derived shoshonitic magma and the

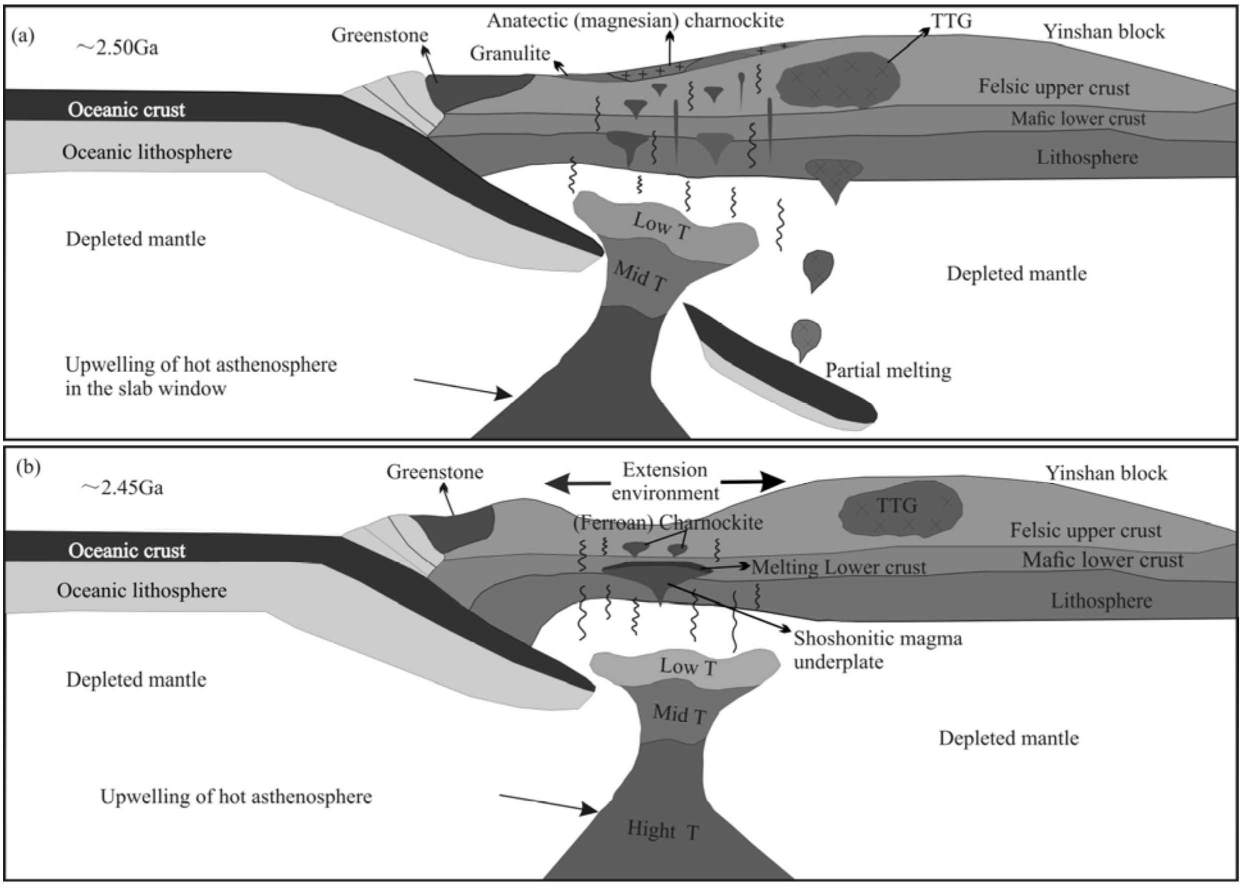

Fig. 19. Proposed tectonic model showing the late Neoarchean subduction–related arc magmatismin from Northern margin of NCC. (a) Maturation of the arc system and emplacement of voluminous Greenstones, TTG and Anatetic Charnockites (~2.5 Ga); (b) the accretion of the arc system to the northern margin of the NCC possibly back–arc basin formation. Upwelling of hot asthenospheric mantle induced the products of Charnockites (~2.45 Ga) by crystal fractionation of associated shoshonitic magma derived from melting of a lithospheric mantle (after Chen et al., 2017).

crystallization differentiation of the melting.

(3) anatectic Magnesian–charnockite might be related to the magmatic island arc environment after subduction of the NCC ~2.5 Ga oceanic crust event, and the anatectic occurred at the post–peak stage of granulite metamorphism. Ferroan–charnockite may be formed by crystallization differentiation of the shoshonitic magma under the ~2.45 Ga back–arc extension environment of collision orogeny.

Acknowledgements

The authors acknowledge the anonymous referees for their constructive suggestions and comments, which helped to improve the paper. This work was financially supported by the National Natural Science Foundation of China (41872194, 41872203).

Manuscript received May 15, 2019
accepted Aug. 14, 2019
associate EIC XIAO Wenjiao
edited by LIU Lian

References

Bai, X., Liu, S.W., Guo, R.R., and Wang, W., 2015., Zircon U–Pb–Hf isotopes and geochemistry of two contrasting Neoarchean charnockitic rock series in eastern Hebei, NCC: Implications for petrogenesis and tectonic setting. Precambrian Research, 267: 72–93.

Barker, F., and Arth, J.G., 1976. Generation of trondhjemitic–tonalitic liquids and Archaean bimodal trondhjemite–basalt suites. Geology, 4: 596–600.

Barrels, R.M., and Mackenzie, F.T., 1971. Evolution of sedimentary rocks. New York: WW Norton and Comp. Inc, 407.

Battacharya, S., and Sen, S.K., 2000. New insights into the origin of Kabbaldurga charnockites, Karnataka, South India. Gondwana Research, 3: 489–506.

Beard, J.S., and Lofgren, G. E., 1991. Dehydration melting and water–saturated melting of basaltic and andesitic greenstones and amphibolites at 1, 3, and 6.9 kbr. Journal of Petrology, 32 (2): 365–40.

Brown, M., 1994. Crustal anatexis and ascent of felsic magmas. Lithos, 32: 109–168.

Brown, M., 2004. The mechanism of melt extraction from the lower continental crust of orogens. Transactions of the Royal Society of Edinburgh, 95: 3–48.

Chacko, T., Ravindra, K.G.R., Meen, J., and Rogers, J.J.W., 1992. Geochemistry of high–grade supracrustal rocks from the Kerala Khondalite Belt and adjacent massif charnockites. Precambrian Research, 55: 469–489.

Cai, J., Liu, F.L., Liu, P.H., and Shi, J.R., 2014. Metamorphic P–T conditions and U–Pb dating of the sillimanite–cordierite–garnet paragneisses in Sanchakou, Jining area, Inner Mongolia. Acta Petrologica Sinica, 30(2): 472–490 (in

Chinese with English abstract).

Chen, L., 2007. Geochronology and geochemistry of the Guyang greenstone belt. Post–Doctor Research Report. Beijing: Institute of Geology and Geophysics. Chinese Academy of Sciences, 1–40 (in Chinese with English abstract).

Chen, N.H.C., Zhao, G.C., Sun, M., and Zhou, H., 2017. Geochemistry of 2.5 Ga granitoids at the northern margin of the Yinshan Block: Implications for the crustal evolution of the NCC. Precambrian Research, 303: 673–686.

Cheng, Y.Q., Yang, C.H., Wan, Y. S., Liu, Z.X., Zhang, X.P., Du, L.L., Zhang, S.G., Wu, J.S., and Gao, J.F., 2004. Early Precambrian geological characters and anatectic reconstruction of crust in North Part of Middle Taihang Mountain. Beijing: Geological Publishing House,191–192 (in Chinese with English abstract).

Condie, K.C., and Allen, P., 1984. Origin of Archaean charnockites from southern India; In: Archaean Geochemistry (eds) A Kröner, G N Hanson and A M Goodwin (Berlin: Springer),183–203.

O'Connor, J.T., 1965. A classification for quartz–rich igneous rocks based on feldspar ratios. U.S, Geological Survey Professional Paper, 525: 79–84.

Dobmeier, C., and Simmat, R., 2002. Post–Grenvillian transpression in the Chilka Lake area, Eastern Ghats Belt d implications for the geological evolution of peninsular India. Precambrian Research, 113: 243–268.

Dong, C.Y., Liu, D.Y., Li, J.J., Wan, Y.S., Zhou, H.Y., Li, C.D., Yang, Y.H., and Xie, L.W., 2007. Palaeoproterozoic Khondalite belt in the western NCC: New evidence from SHRIMP dating and Hf isotope composition of zircons from metamorphic rocks in the Bayan Ul–Helan Mountains area. Chinese Science Bulletin, 52(21): 2984–2994.

Dong, C.Y., Wan, Y.S., Xu, Z.Y., Liu, D.Y., Yang, Z.S., Ma, M.Z., and Xie, H.Q., 2013. SHRIMP zircon U–Pb dating of Late Paleoproterozoic kondalites in the Daqing Mountains area on the NCC. Science China Earth Sciences, 56(1): 115–125.

Dong, X.J., Xu, Z.Y., Liu, Z.H., and Qian, S., 2012a. Zircon U–Pb geochronology of Archean high–grade metamorphic rocks from Xi Ulanbulang area, central Inner Mongolia. Science in China (Earth Sciences), 5: 204–212.

Dong, X.J., Xu, Z.Y., Liu, Z.H., and Sha, Q. 2012b. 2.7 Ga Granitic gneiss in the northern foot of Daqingshan Mountain, Central Inner Mongolia, and its geological implications. Earth Science, 37: 20–27 (in Chinese with English abstract).

Drummond, M.S., and Defant, M.J.,1990. A model for trondhjemite–tonalite–dacite genesis and crustal growth via slab melting: Archaean to modern comparisons. Journal of Geophysical Research, 95: 21503–2152.

Eggler, D.H., 1987. Solubility of major and trace elements in mantle metasomatic fluids: experimental constraints. In: Mantle metasomatism, Menzies, M.A., and Hawkesworth, C.J. (eds) (London: Academic Press), 21–41.

Emslie, R.F., 1991. Granitoids of rapakivi granite–anorthosite and related associations. Precambrian Research, 51(1–4): 173–192.

Fowler, M.B., Henney, P.J., Darbyshire, D.P.F., and Greenwood, P.B., 2001. Petrogenesis of high Ba - Sr granites: The Rogart pluton, Sutherland.Journal of Geological Society of London, 158(3): 521–534.

Frost, B.R., Frost, C.D., Hulsebosch, T.P., and Swapp, S.M., 2000. Origin of the charnockites of the Louis lake Batholith, wind River Range, Wyoming. Journal of Petrology, 41(12): 1759–1776.

Frost, B.R., Barnes, C.G., Collins, W.J., Arculus, R.J., Ellis, D.J., and Frost, C.D., 2001. A geochemical classification for granitic rocks. Journal of Petrology, 42(11): 2033–2048.

Frost, B.R., and Frost, C.D., 2008. On charnockites. Gondwana Research, 13(1): 30–44.

Gao, S., and Jin, Z.M., 1997. Delamination and its geodynamical significance for the crust mantle evolution. Geological Science and Technology Information, 16(1): 1–9 (in Chinese with English abstract).

Gao, S., 1999. Discussions on some problems in research into chemical compositions of continental crust. Earth Science, 24 (3): 228–233 (in Chinese with English abstract).

Geisler, T., Schaltegger, U., and Tomaschek, F., 2007. Re–equilibration of zircon in aqueous fluids and melts. Elements, 3(1): 43–50.

Geng, Y.S., Shen, Q.H., and Chen, T., 1990. Geochemistry and origin of charnockites in Qianan–Qianxi area, eastern Hebe. Acta Petrologica et Mineralogica, 9(3): 193–202 (in Chinese with English abstract).

Geng, Y.S., Shen, Q.H., Du, L.L., and Song, H.X., 2016. Regional metamorphism and continental growth and assembly in China. Acta Petrologica Sinica, 32(9): 2579–2608 (in Chinese with English abstract).

Guo, J.H., Wang, S.S., Sang, H., and Zhai, M.G., 2001.^{40}Ar–^{39}Ar age spectra of garnet Porphyroblast: Implications for metamorphic age of high–pressure granulite in the NCC. Acta Petrologica Sinica, 17(3): 436–442 (in Chinese with English abstract).

Guo, J.H., Peng, P., Chen, Y., Jiao, S.J., and Windley, B.F., 2012. UHT Sapphirine granulite metamorphism at 1.93–1.92 Ga caused by gabbronorite intrusions: Implications for tectonic evolution of the northern margin of the NCC. Precambrian Research, 222–223: 124–142.

Gordon, S.M., Whitney, D.L., Teyssier, C., and Fossen, H., 2013. U–Pb dates and trace–element geochemistry of zircon from migmatite, Western Gneiss Region, Norway: Significance for history of partial melting in continental subduction. Lithos, 170–171: 35–53.

Han, X., Pei, L., Zheng, Y.Y., and Liu, J.L., 2016. Zircon U–Pb geochronology and geochemistry of charnockitic rocks from Qian'an in the northern part of NCC: Implications for petrogenesis and tectonic setting. Acta Petrologica Sinica, 32 (9): 2823–2838.

Hansen, E.C., Janardhan, A.S., Newton, R.C., Prame, W.K.B.N., and Kumar, G.R.R., 1987. Arrested charnockite formation at Kabbaldurga. South India. Nature, 278: 511–514.

Harlov, D.E., 2012. The potential role of fluids during regional granulite–facies dehydration in the lower crust. Geoscience Frontiers, 3(6), 813–827.

Hidaka, H., Shimizu, H., and Adachi, M., 2002. U–Pb geochronology and REE geochemistry of zircons from Palaeoproterozoic paragneiss clasts in the Mesozoic Kamiaso conglomerate, central Japan: Evidence for an Archean provenance. Chemical Geology, 187(3–4): 279–29.

Holland, T.H., 1900. The charnockite series, a group of Archean hypersthenic rocks in peninsular India. Memoirs of the Geological Survey of India, 28: 119–249.

Hoskin, P.W.O., and Schaltegger, U., 2003. The composition of zircon and igneous and metamorphic petrogenesis. Reviews in Mineralogy and Geochemistry, 53(1): 27–62.

Janardhan, A.S., Newton, R.C., and Hansen, E.C., 1982. The transformation of amphibolite facies gneiss to charnockite in southern Karnataka and northern Tamil Nadu, India. Contributions to Mineralogy and Petrology, 79(2): 130–149.

Jin, W., Li, S.X., and Liu, X.S., 1991. A study on characteristics of Early Precambrian high–grade metamorphic rock series and their metamophic dynamics. Acta Petrologica Sinica, 7(4): 27–35 (in Chinese with English abstract).

Jin, W., Li, S.X., 1994. The lithological association and geological features of Early Proterozoic orogenic belt in Daqingsha, Inner Mongolia. In: Qian XL and Wang RM (ed). Geological Evolutionof the Granulite Terrain in North Part of the NCC, Beijing: Seismological Press (in Chinese with English abstract).

Jia, H.Y., Hao, J.F., and Xu, L.Q., 2004. Structural styles and evolution of Archean high–grade metamorphic region in central Inner Mongolia. Geology and mineral resources of South China, 1: 35–38 (in Chinese with English abstract).

Jian, P., Zhang, Q., Liu, D.Y., Jin, W.J., Jia, X.Q., and Qian, Q., 2005. SHRIMP dating and geological significance of Late Achaean high–Mg diorite(sanukite) and hornblende–granite at Guyang of Inner Mongolia. Acta Petrologica Sinica, 21(1): 151–157 (in Chinese with English abstract).

Jian, P., Liu, D., Kröner, A., Windley, B.F., Shi, Y., Zhang, F., Shi, G., Miao, L., Zhang, W., Zhang, Q., Zhang, L., and Ren, J., 2008. Time scale of an early to mid–Paleozoic orogenic cycle of the long–lived Central Asian Orogenic Belt, Inner Mongolia of China: implications for continental growth. Lithos, 101: 233–259.

Jian, P., Kröner, A., Windley, B.F., Zhang, Q., Zhang, W., and Zhang, L.Q., 2012. Episodic mantle melting–crustal reworking in the late Neoarchean of the northwestern NCC: zircon ages of magmatic and metamorphic rocks from the Yinshan Block. Precambrian Research, 222–223: 230–254.

Johnson, K.T.M., 1998. Experimental determination of partition coefficients for rare earth and high–field–strength elements between clinopyroxene, garnet, and basaltic melt at high pressures. Contributions to Mineralogy & Petrology, 133(1–2): 60–68.

Kar, R., Bhattacharya, S., and Sheraton, J.W., 2003. Hornblende –dehydration melting in mafic rocks and the link between massif–type charnockite and associated granulites, Eastern Ghats Granulite Belt, India. Contributions to Mineralogy and Petrology, 145(6): 707–729.

Kriegsman, L.M., 2001. Partial melting, partial melt extraction and partial back reaction in anatectic migmatites: Lithos, 56 (1): 75–96.

Kaszuba, J.P., and Wendlandt, R.F., 2000. Effect of carbon dioxide on dehydration melting reactions and melt compositions in the lower crust and the origin of alkaline rocks. Journal of Petrology, 4: 363–386.

Keppie, J.D., Dostal, J., Cameron, K.L., Solari, L.A., Ortega, G., and Lopez, R., 2003. Geochronology and geochemistry of Grenvillian igneous suites in the northern Oaxacan Complex, southern Mexico: tectonic implications. Precambrian Research, 120: 365–389.

Le, Maitre, R.W., 2002. Igneous Rocks. A Classification and Glossary of Terms. Recommendations of the International Union of Geological Sciences Subcommission on the Systematics of Igneous Rocks, 2nd Edition, Cambridge: Cambridge University Press, 130–171 (in Chinese with English abstract).

Li, J.H., Qian, X.L., and Liu, S.W., 2000. Geochemistry of Khondalites from the central portion of NCC (NCC): implications for the continental cratonization in the Neoarchean. Science in China (Earth Sciences), 43(3): 253–265 (in Chinese with English abstract).

Li, X.P., Yang, Z.Y., Zhao, G.C., Grapes, R., and Guo, J.H., 2011. Geochronology of Khondalite–series rocks of the Jining complex: Confirmation of depositional age and tectonometamorphic evolution of the NCC. International Geology Review, 53(10): 1194–1211.

Li, S., and Zhao, G., 2007. Shrimp U–Pb zircon geochronology of the liaoji granitoids: constraints on the evolution of the paleoproterozoic Jiao–Liao–Ji belt in the eastern block of the NCC. Precambrian Research, 158(1): 1–16.

Litvinovsky, B.A., Steele, I.M., and Wickham, S.M. 2000. Silicic magma formation in overthickened crust: Melting of charnockite and leucogranite at 15, 20 and 25 kbar. Journal of Petrology, 41: 717–737.

Liu, J.H., Liu, F.L., Ding, Z.J., Liu, P.H., Chen, J.Q., Liu, C.H., Wang, F., Yang, H., Cai, J., and Shi, J.R., 2017. Late Neoarchean–Paleoproterozoic arc–continent accretion along the Khondalite Belt, Western Block, NCC: Insights from granitoid rocks of the Daqingshan–Wulashan area. Precambrian Research, 303: 494–519.

Liu, P.H., Liu, F.L., Cai, J., Liu, J.H., Shi, J.R., and Wang, F., 2013. Geochronological and geochemical study of the Lijiazi mafic granulites from the Daqingshan–Wulashan metamorphic complex, the central Khondalite Belt in the NCC. Acta Petrologica Sinica, 29(2): 462–484 (in Chinese with English abstract).

Liu, J.H., Liu, F.L., Ding, Z.J., Liu, P.H., Chen, J.Q., Liu, C.H., Wang, F., Yang, H., Cai, J., and Shi, J.R., 2017. Late Neoarchean–Paleoproterozoic arc–continent accretion along the Khondalite Belt, Western Block, NCC: Insights from granitoid rocks of the Daqingshan–Wulashan area. Precambrian Research, 303: 497–519.

Liu, L., Zhang, L.C., and Dai, Y.P., 2012. Formation age, geochemical and geological significance of the Sanheming BIF–type iron deposit in the Guyang greenstone belt, Inner Mongolia. Acta Petrologica Sinica, 28(11): 3623–3637 (in Chinese with English abstract).

Lu, L.Z., Jin, S.Q., Xu, X.C., and Liu, F.L., 1992. The Petrogenesis and Ore–bearing Potential of Precambrian Khondalite Series in Southeast Inner Mongolia. Changchun: Jilin Science and Technology Press, 4–121 (in Chinese with English abstract).

Lu, L.Z., and Jin, S.Q., 1993. P–T–t paths and tectonic history of an Early Precambrian granulite facies terrane, Jining district, south–east Inner Mongolia, China. Journal of Metamorphic Geology, 11(4): 483–498.

Ma, M.Z., Dong, C.Y., Xu, Z.Y., Xie, S.W., Liu, D.Y., and Wan, Y.S., 2015. Anatexis of Early Paleoproterozoic garnet–biotite gneisses (Daqingshan supracrustal rocks) in Daqingshan, Inner Mongolia: Geology, zircon geochronology and geochemistry. Acta Petrologica Sinica, 31(6): 1535–1548 (in Chinese with English abstract).

Ma, X.D., Guo, J.H., Chen, L., and Chu, Z.Y., 2010. Re–Os isotopic constraint to the age of komatiites in the Neoarchean Guyang greenstone belt: NCC. Chinese Sci Bull, 55(27–28): 3197–3204.

Ma, X.D., Fan, H.R., Santosh, M., and Guo, J.H., 2013a. Geochemistry and zircon U–Pb chronology of charnockites in the Yinshan Block, NCC: Tectonic evolution involving Neoarchaean ridge subduction. International Geology Review, 55(13): 1688–1704.

Ma, X.D., Fan, H.R., Santosh, M., and Guo, J.H., 2013b. Geochemistry and zircon U–Pb chronology of charnockites in the Yinshan Block, NCC: Tectonic evolution involving Neoarchaean ridge subduction. International Geology Review, 55(13): 1688–1704.

Ma, X.D., Fan, H.R., and Guo, J.H., 2013c. Neoarchean magmatism, metamorphism in the Yinshan Block: Implication for the genesis of BIF and crustal evolution. Acta Petrologica Sinica, 29(7): 2329–2339 (in Chinese with English abstract).

Ma, X.D., Fan, H.R., Santosh, M., and Guo, J.H., 2016. Petrology and geochemistry of the Guyang hornblendite complex in the Yinshan block, NCC: Implications for the melting of subduction–modified mantle. Precambrian research, 273: 38–52.

Martin, H., 1986. Effect of steeper Archaean geothermal gradient on geochemistry of subduction–zone magmas. Geology, 14: 753–756.

Montel, J.M., and Vielzeuf, D., 1997. Partial melting of meta–greywackes, Part II. Compositions of minerals and melts. Contrib Mineral Petrol, 128:176–196.

Nagasawa, H., 1970. Rare earth concentrations in zircons and apatites and their host dacites and granites. Earth and Planetary Science Letters, 9(4): 359–364.

Patiño, Douce.A.E., 1997. Generation of metaluminous A–type granites by low–pressure melting of calc–alkaline granitoids. Geology, 25: 743–746.

Patiño, Douce.A.E., and Beard, J. S., 1995.Dehydration melting of biotite gneiss and quartz amphibolite from 3 to 15 kbar. Journal of Petrology, 36: 707–738.

Peccerillo, A., and Talor, S.R., 1976. Geochemistry of Eocene calc alkaline volcanicrocks from the Kastomononarea, northern Turkey. Contributions to Mineralogy and Petrology, 58: 63–81.

Percival, J.A., Stern, R.A., and Rayner, N., 2003. Archean adakites from the Ashuanipi complex, eastern Superior Province, Canada: geochemistry, geochronology and tectonic significance. Contributions to Mineralogy & Petrology, 145 (3): 265–280.

Peng, P., Guo, J.H., Windley, B.F., Liu, F., Chu, Z., and Zhai, M.G., 2012. Petrogenesis of Late Paleoproterozoic Liangcheng charnockites and S–type granites in the central–northern margin of the NCC: Implications for ridge subduction. Precambrian Research, 222–223: 107–123.

Qian, X.L., Cui, W.Y., Wang, S.Q., and Wang, G.Y., 1985. Geology of Precambrian Iron Ores in Eastern Hebei Province. China. Shijiazhuang: Hebei Science and Technology Press, 273 (in Chinese with English abstract).

Qian, Q., Cheng, S.L., Li, T.Y., and Wen, D.J., 2003. Mesozoic high Ba–Sr granitoids from North China: Geochemical

characteristics and geological implications. Terra Nova, 15(4): 272–278.
Rapp, R.P., Watson, E.B., and Miller, C.F., 1991. Partial melting of amphibolite/eclogites and the origin of Archean trondhjemites and tonalites. Precambrian Research, 51(1–4): 1–25.
Rapp, R.P., and Watson, E.B., 1995. Dehydration melting of metabasalt at 8–32kbar: Implications for continental growth and crust–mantle recycling. Journal of Petrology, 36(4): 891–931.
Raith, M., and Srikantappa, C., 1993. Arrested charnockite formation at Kottavattom, southern India. Journal of Metamorphic Geology, 11(6): 815–832.
Rajesh, H.M., and Santosh, M., 2004. Charnockitic magmatism in southern India. Journal of Earth System Science, 113(55): 565–585.
Rajesh, H.M., Santosh, M., and Yoshikura, S., 2011. The Nagercoil charnockite: a magnesian, calcic to calc–alkalic granitoid dehydrated during a granulite–facies metamorphic event. Journal of Petrology, 52: 375–400.
Rajesh, H.M., 2012. A geochemical perspective on charnockite magmatism in Peninsular India. Geoscience Frontiers, 3(6): 773–788.
Rajesh, H.M., and Santosh, M., 2012. Charnockites and charnockites. Geoscience Frontiers, 3(6): 737–744.
Rajesh, H.M., 2007. The petrogenetic characterization of intermediate and silicic charnockites in high–grade terrains: A case study from southern India. Contributions to Mineralogy and Petrology, 154(5): 591–606.
Ren, Y.W., 2010. The study of granite–greenstone belt in Xihongshan area, Inner Mongolia. Master Degree Thesis. Changchun: Jilin University1 (Ph. D thesis): 1–69 (in Chinese with English abstract).
Rushmer, T., 1991. Partial melting of two amphibolites: Contrasting experimental results under fluid–absent conditions. Contributions to Mineralogy and Petrology, 107 (1): 41–59.
Rubatto, D., Gebauer, D., and Compagnoni, R., 1999. Dating of eclogite–facies zircons: The age of Alpine metamorphism in the Sesia–Lanzo Zone (Western Alps). Earth and Planetary Science Letters, 167(3–4), 141–158.
Rubatto, D., 2002. Zircon trace element geochemistry: Partitioning with garnet and the link between U–Pb ages and metamorphism. Chemical Geology, 184(1–2): 123–138.
Springer, W., and Seck, H.A., 1997. Partial fusion of basic granulites at 5 to 15 kbar: implications for the origin of TTG magmas. Contributions to Mineralogy and Petrology, 127: 30–45.
Su, S.G., Deng, J.F., Liang, F.H., Zhou, X.R., and Gu, D.L., 2003. Occurenee of the restite mineral in charnockites and the prosses of charnockites formation in Yin Shan area, Shan Dong Province. Earth Science Frontiers, 10(3): 257–267 (in Chinese with English abstract).
Sun, S.S., and McDough, W.F., 1989. Chemical and isotopic systematics of oceanic basalts: Implications for mantle composition and processes. In: Saunders, A.D., and Norry, M.J., (eds.). Magmatism in the Ocean Basins. Geological Society of London, 42: 313–345.
Shi, Q., Dong, X.J., Xu, Z.Y., Guan, Q.B., Li, P.C., Zhang, C., and Cui, F.H., 2018. Anatectic origin and geological significance of the Paleoproterozoic gneissic garnet granite in the Jining area, northern margin of the NCC. Acta Petrologica Sinica, 34(9): 2754–2772 (in Chinese with English abstract).
Shi, Q., Xu, Z.Y., Dong, X.J., Li, P.C., Wang, S.J., Li, C.H., 2019a. Petrogenesis and geological significance of charnockite in the Yinshan Block of NCC. International Geology Review, 61(7): 895–913.
Shi, Q., Fan, Z.W., Dong, X.J., Xu, Z.Y., Li, P.C., Wang, S.J., Li, C.H., 2019b. Anatectic origin and geological significance of the Neoarchean ~2.5 Ga charnockite in the Jining area, northern North China Craton. Geological Journal, 54: 2731–2753.
Shi, Q., Xu, Z.Y., Dong, X.J., Liu, Z.H., and Li, S.C., 2019c. SHRIMP U–Pb Geochronology of Zircon in the North China Craton: Revealing Late Archean Tectonic Events in the Jining Area. Acta Geologica Sinica (English Edition), 93(4): 1146–1148.
Stahle, H.J., Raith, M., Hoernes, S.,and Delfs, A., 1987. Element mobility during incipient granulite formation at Kabbaldurga, southern India. Journal of Petrology, 28(5): 803–834.
Santosh, M., and Yoshida, M., 1992. A petrologic and fluid inclusion study of charnockites from the Lützow–Holm Bay region, East Antarctica: Evidence for fluid–rich metamorphism in the lower crus. Lithos, 29(1–2): 107–126.
Santosh, M., Sajeev, K., Li, J.H., 2006. Extreme crustal metamorphism during Columbia supercontinent assembly: Evidence from NCC. Gondwana Research, 10(3–4): 256–266.
Santosh, M., Tsunogae, T., Li, J.H., and Liu, S.J., 2007a. Discovery of sapphirine–bearing Mg–Al granulites in the NCC: Implications for Paleoproterozoic ultrahigh temperature metamorphism. Gondwana Research, 11(3): 263–285.
Santosh, M., Wilde, S.A., and Li, J.H., 2007b. Timing of Paleoproterozoic ultrahigh–temperature metamorphism in the NCC: evidence from SHRIMP U–Pb zircon geochronology. Precambrian Research, 159(3–4): 178–196.
Sisson, W.T., Ratajeski, K., Hankins, B.W., and Glazner, A., 2005. Voluminous granitic magmas from common basaltic sources. Contributions to Mineralogy and Petrology, 148(6): 635–661.
Santosh, M., Tagawa, M., Taguchi, S., and Yoshikura, S., 2003. The Nagercoil Granulite Block, southern India: petrology,fluid inclusions and exhumation history. Journal Asian Earth Science, 22: 131–155.
Skjerlie, K.J., and Johnston, A.D., 1993. Fluid–absent melting behavior of an F–rich tonalitic gneiss ar mid–crustal pressures: implications for the generation of anorogenic granites. Journal of Petrology, 34: 785–815.
Song, H.F., Xu, Z.Y., and Liu, Z.H., 2005. Geochemical characteristics and origin of garnet migmatitic granites in Daqingshan area, Inner Mongolia. Acta Petrologica et Mineralogica, 24(5): 489–495 (in Chinese with English abstract).
Stuckless, J.S., and Irving, A.J., 1976. Strontium isotope geochemistry of megacrysts and host basalts from southeastern australia. Geochimica et Cosmochimica Acta, 40 (2): 209–213.
Scoates, J.S., Frost, C.D., Mitchell, J.N., Lindsley, D.H., and Frost, B.R., 1996. Residual–liquid origin for a monzonite intrusion in a mid–Proterozoic anorthosite complex: the Sybille intrusion, Laramie anorthosite complex, Wyoming. Geological Society of America Bulletin, 108: 1357–1371.
Srikantappa, C., 1996. The Nilgiri granulites. Gondwana Research Group Memoir, 3: 185–222.
Tao, J.X., and Hu, F.X., 2002, The formation of the garnet–bearing migmatitic granite in Zhuozishan Area, Inner Mongolia, China. Progress in Precambrian Research, 25(1): 59–64 (in Chinese with English abstract).
Tarney, J., 1976. Geochemistry of Archaean high–grade gneisses with implications as to the origin and evolution of the Precambrian crust. In: The early history of the Earth. Windley, B.F., (ed) (London: Wiley): 405–417.
Wan, Y.S., Wilde, S.A., Liu, D.Y., Yang, C.X., Song, B., Yin, X.Y., 2006. Further evidence for 1.85 Ga metamorphism in the Central Zone of the NCC: SHRIMP U–Pb dating of zircon from metamorphic rocks in the Lushan area, Henan Province. Gondwana Research, 9(1–2): 189–197.
Wan, Y.S., Liu, D.Y., Xu, Z.Y., Dong, C.Y., Wang, Z.J., Zhou, H.Y., Yang, Z.S., Liu, Z.H., and Wu, J.S., 2008. Paleoproterozoic crustally derived carbonate-rich magmatic rocks from the Daqinshan area, North China Craton: Geological, petrographical, geochronological and geochemical (Hf, Nd, O and C) evidence. American Journal of Science, 308: 351–378.
Wan, Y.S., Liu, D.Y., Dong, C.Y., Liu, S.J., Wang, S.J., and Yang, E.X., 2011. U-Th-Pb behavior of zircons under high-grade metamorphic conditions: A case study of zircon dating of meta-diorite near Qixia, eastern Shandong. Geoscience Frontiers, 2: 137–146.
Wan, Y.S., Liu, D.Y., Dong, C.Y., Xu, Z.Y., Wang, Z.J., Wilde, S.A., Yang, Y.H., Liu, Z.H., and Zhou, H.Y., 2009. The

Precambrian khondalite belt in the Daqingshan area, NCC: Evidence for multiple metamorphic events in the Palaeoproterozoic era. In: Reddy SM, Mazumder R, Evans DAD and Collins AS (eds.). Palaeoproterozoic Supercontinents and Global Evolution. Geological Society London, Special Publications, 323(1): 73–97.

Wan, Y.S., Xu, Z.Y., Dong, C.Y., Nutman, A., Ma, M.Z., Xie, H.Q., Liu, S.J., Liu, D.Y., Wang, H.C., and Cu, H., 2013a. Episodic Paleoproterozoic (~2.45, ~1.95 and ~1.85 Ga) mafic magmatism and associated high temperature metamorphism in the Daqingshan area, NCC: SHRIMP zircon U–Pb dating and whole–rock geochemistry. Precambrian Research, 224: 71–93.

Wan, Y.S., Xie, H.Q., Yang, H., Wang, Z.J., Liu, D.Y., Kroner, A., Wilde, S.A., Geng, Y.S., Sun, L.Y., Ma, M.Z., Liu, S.J., Dong, C.Y., and Du, L.L., 2013b. Is the Ordos Block Archean or Paleoproterozoic in age? Implications for the Precambrian evolution of the North China Craton. American Journal of Science, 313: 683–711.

Wan, Y.S., Liu, D.Y., Dong, C.Y., Xie, H.Q., Kröner, A., Ma, M.Z., Liu, S.J., Xie, S.W., and Ren, P., 2015. Formation and evolution of Archean continental crust of the North China Craton. In: Zhai MG (Ed.) Precambrian geology of China. Springer, 59–136.

Wang, K.Y., Bai, Y.L., Yang, R.Y., and Huang, Z.X., 1984. Rare earth element geochemistry of Qianan charnockite. Scientia Geologica Sinica, 3(9): 330_340 (in Chinese with English abstract).

Wang, A.J., 1992. Geochemistry and genesis of the sodium–charnockitic gneisses, eastern Hebei Province, China. Acta Geologica Sinica, 66(1): 15–34 (in Chinese with English abstract).

Wang, C., Song, S.G., Niu, Y.L., and Su, L., 2015. Late Triassic Adakitic plutons within the Archean terrane of the NCC: Melting of the ancient lower crust at the onset of the lithospheric destruction. Lithos, 212–215: 353–367.

Wang, H.C., Lu, S.N., Zhao, F.Q., and Zhong, C.T., 2005. The Paleoproterozoic geological records in NCC and their tectonic significance. Geological Survey and Research, 28(3): 129–143 (in Chinese with English abstract).

Weaver, B.L., 1980. Rare–earth element geochemistry of Madras granulites. Contributions to Mineralogy & Petrology, 71: 271–279.

Wilson, M. J., 1989.Igneous Petrogenesis. London: Unwin Hyman, 552.

Xu, Z.Y., Liu, Z.H., Dong, X.J., Dong, C.Y., and Wan, Y.S., 2011. Discovery of kyanite garnet quartz feldspathic gneiss in the north side of Daqing Mts, Inner Mongolia, and its petrography, geochemistry and zircon SHRIMP dating. Geological Review, 57(2): 243–252 (in Chinese with English abstract).

Xu, Z.Y., Fan, Z.W., Liu, Z.H., Li, S.C., Wang, W.Q., Zhang, C., Ma, Y., and Wang, Y.N., 2013. Formation age of the marble in the khondalite series in Jining, Inner Mongolia: Evidence of the LA–ICP–MS zircon U–Pb dating of felsic gneiss. Journal of Jilin University (Earth Science Edition), 43(3): 809–819 (in Chinese with English abstract).

Xu, Z.Y., Wan, Y.S., Dong, C.Y., Ma, M.Z., and Liu, D.Y., 2015. Late Neoarchean magmatism identified in Daqingshan, Inner Mongolia: SHRIMP zircon U–Pb dating. Acta Petrologica Sinica, 31(6):1509–1517.

Yang, Q.Y., Santosh, M., and Tsunogae, T., 2014. First report of Paleoproterozoic incipient charnockite from the NCC: Implications for ultrahigh–temperature metasomatism. Precambrian Research, 243: 168–180.

Yang, Q.Y., Santosh, M., Collins, A.S., and Teng, X.M., 2016, Microblock amalgamation in the NCC: Evidence from Neoarchaean magmatic suite in the western margin of the Jiaoliao Block: Gondwana Research,31: 96–123.

Ye, H.M., Li, X.H., Li, Z.X., and Zhang, C.L., 2008. Age and origin of high Ba–Sr appinite–granites at the northwestern margin of the Tibet Plateau: Implications for early Paleozoic tectonic evolution of the Western Kunlun orogenic belt. Gondwana Research,13(1): 126–138.

Yoshida, M., Funaki, M., and Vitanage, P.W., 1992. Proterozoic to Mesozoic East Gondwana: the juxtaposition of India–Sri Lanka–Antarctica. Tectonocs II, 11(2): 392–404.

Young, D.N., Zhao, J.X., Ellis, D.J., and Mcculloch, M.T., 1997, Geochemical and Sr–Nd isotopic mapping of source provinces for the Mawson charnockites, east Antarctica: implications for Proterozoic tectonics and Gondwana reconstruction. Precambrian Research. 86(1–2): 1–19.

Zhang, X.H., Yuan, L.L., Xue, F.H., and Zhai, M.G., 2014. Neoarchean metagabbro and charnockite in the Yinshan block, western NCC: Petrogenesis and tectonic implications. Precambrian Research, 255(2): 563–582.

Zhang, Z.Q., Wang, Q., Wei, Y.S., Liu, C.R., Yang, W.B., Duan, C.S., and Yang, Y.H., 2017. Main achievements in supplemental regional geological survey of 1: 250000 Datong Sheet. Geological Survey of China, 4(4): 50–59 (in Chinese with English abstract).

Zhang, Y.Q., Xu, L.Q., Jia, H.Y., Liu, Y.F., and Wang, T., 2005. Metamorphic petrology and tectonic setting of the Xiulanbulang high–grade terrain, Wuchuan County, Inner Mongolia. Geological Survey and Research, 28: 71–78 (in Chinese with English abstract).

Zhao, G.C., Wilde, S.A., Cawood, P.A., and Lu, L.Z., 1998. Thermal evolution of the Archean basement rocks from the eastern part of the NCC and its bearing on tectonic setting. International Geology Reviews, 40: 706–721.

Zhao, G.C., Wilde, S.A., Cawood, P.A., and Lu, L.Z., 1999. Tectonothermal history of the basement rocks in the western zone of the NCC and its tectonic implications. Tectonophysics, 310(1–4): 37–53.

Zhao, G.C., Sun, M., and Wilde, S.A., 2003. Major tectonic units of the NCC and their Paleoproterozoic assembly. Science in China (Earth Science), 46(1): 23–38.

Zhao, G.C., Sun, M., Wilde, S.A., Li, S.Z., 2005. Late Archean to Paleoproterozoic evolution of the NCC: Key issues revisited. Precambrian Research, 136(2): 177–202.

Zhao, L., Li, T.S., Peng, P., Guo, H.J., Wang, W., Wang, H.Z., Santosh, M., and Zhai, M.G., 2015. Anatomy of zircon growth in high pressure granulites: SIMS U–Pb geochronology and Lu–Hf isotopes from the Jiaobei Terrane, eastern NCC. Gondwana Research, 28(4): 1373–1390.

About the first author

SHI Qiang, male, born in 1992 in Anshan City, Liaoning Province; doctoral candidate; study in Jilin University; research assistant of structural geology, College of Earth Sciences of Jilin University. He is now interested in the study on Early Precambrian metamorphic tectonic evolution, and garnet-bearing granite. Email: 1130025711@qq.com; phone: 13578720423.

About the corresponding author

XU Zhongyuan, male, born in 1958 in Datong City, Shanxi Province; master; graduated from Jilin University; research assistant of structural geology, College of Earth Sciences of Jilin University. He is now interested in the study on Early Precambrian metamorphic tectonic evolution of North China Craton. E-mail: xuzy@jlu.edu.cn; phone: 13844161972.